Journal of Inorganic Biochemistry 247 (2023) 112326

Contents lists available at ScienceDirect

Journal of Inorganic Biochemistry

journal homepage: www.elsevier.com/locate/jinorgbio

Carbohydrate effect of novel arene Ru(II) phenanthroline-glycoconjugates on metastatic biological processes

Elena de la Torre-Rubio [a], Laura Muñoz-Moreno [b], Ana M. Bajo [b], Maria-Selma Arias-Pérez [a], Tomás Cuenca [a], Lourdes Gude [a], Eva Royo [a,*]

[a] Universidad de Alcalá, Instituto de Investigación Química "Andrés M. del Río" (IQAR), Departamento de Química Orgánica y Química Inorgánica, 28805 Alcalá de Henares, Madrid, Spain

[b] Universidad de Alcalá, Facultad de Medicina y Ciencias de la Salud, Departamento de Biología de Sistemas, 28805 Alcalá de Henares, Madrid, Spain

ARTICLE INFO

Keywords:
Arene-ruthenium
Antimetastatic
Metal glycoconjugates
MMP inhibitors
Carbohydrate
Antimigratory

ABSTRACT

Novel water-soluble half-sandwich ruthenium(II) polypyridyl-glycoconjugates [Ru(p-cymene)Cl{*N*-(1,10-phenanthroline-5-yl)-β-glycopyranosylamine}][Cl] (glycopyranosyl = D-glucopyranosyl (**1**), D-mannopyranosyl (**2**), L-rhamnopyranosyl (**3**) and L-xylopyranosyl (**4**)) have been synthesized and fully characterized. Their behaviour in water under physiological conditions has been studied by nuclear magnetic resonance spectroscopy, revealing their hydrolytic stability. Interactions of the novel compounds with duplex-deoxiribonucleic acid (dsDNA) were investigated by different techniques and the results indicate that, under physiological pH and saline conditions, the metal glycoconjugates bind DNA in the minor groove and/or through external, electrostatic interactions, and by a non-classical, partial intercalation mechanism in non-saline phosphate buffered solution. Effects of compounds **1**–**4** on cell viability have been assessed in vitro against two human cell lines (androgen-independent prostate cancer PC-3 and non-tumorigenic prostate RWPE-1), showing moderate cytotoxicities, with IC_{50} values higher than those found for free ligands [*N*-(1,10-phenanthroline-5-yl)-β-glycopyranosylamine] (glycopyranosyl = D-glucopyranosyl (**a**), D-mannopyranosyl (**b**), L-rhamnopyranosyl (**c**) and L-xylopyranosyl (**d**)) or corresponding metal-aglycone. Cell viability was assayed in the presence and absence of the glucose transporters (GLUTs) inhibitor [N^4-{1-(4-cyanobenzyl)-5-methyl-3-(trifluoromethyl)-1*H*-pyrazol-4-yl}-7-fluoroquinoline-2,4-dicarboxamide] (BAY-876), and the results point to a negligible impact of the inhibition of GLUTs on the cytotoxicity caused by Ru(II) compounds **1**–**4**. Remarkably, glycoconjugates **1**–**4** potently affect the migration pattern of PC-3 cells, and the wound healing assay evidence that the presence of the carbohydrate and the Ru(II) center is a requisite for the anti-migratory activity observed in these novel derivatives. In addition, derivatives **1**–**4** strongly affect the matrix metalloproteinase MMP-9 activities of PC-3 cells, while proMMP-2 and especially proMMP-9 were influenced to a much lesser extent.

Abbreviations: ABB, Annexin Binding Buffer; APT, Attached Proton Test; BAY-876, [N^4-{1-(4-cyanobenzyl)-5-methyl-3-(trifluoromethyl)-1*H*-pyrazol-4-yl}-7-fluoroquinoline-2,4-dicarboxamide]; BPC grade, Biotechnology Performance Certified grade; Cisplatin, *cis*-[$PtCl_2(NH_3)_2$]; COSY, Correlation Spectroscopy; Cq, Quaternary carbon; CT, Calf Thymus; DMSO, dimethylsulfoxide; DMEM, Dulbecco's Modified Eagle's Medium; Duplex, ds; DNA, Deoxyribonucleic acid; EDTA, ethylendiaminetetraacetic acid; ELISA, Enzyme-Linked Immuno Sorbent Assay; FAM, 6-carboxyfluorescein; FBS, Fetal Bovine Serum; FRET, Fluorescence Resonance Energy Transfer; FT, Fourier Transform; F10T, 5'-FAM-AGC TAT TA TA /sp18/ TA TA GCT ATA-TAMRA-3'; HSQC, Heteronuclear Single Quantum Coherence spectroscopy; HMBC, Heteronuclear Multiple Bond Correlation spectroscopy; HPLC, High Performance Liquid Chromatography; ICP-OES, Inductively Coupled Plasma optical Emission Spectroscopy; IDT, Integrated DNA Technologies; IR, Infrared; MMPs, matrix metaloproteinases; MMP-2, matrix metaloproteinase-2; MMP-9, matrix metaloproteinase-9; MTT, 3-(4,5-dimethylthiazol-2-yl)-2,5-diphenyltetrazolium bromide; NMR, Nuclear magnetic resonance; PAGE, PolyAcrylamide Gel Electrophoresis; PBS, Phosphate buffered saline solution; PC-3, Human androgen-independent prostate cancer cell line; RAPTA-C, [$RuCl_2(\eta^6$-p-cymene)(PTA)] (PTA = 1,3,5-triaza-7-phosphoadamantane; RPMI, Roswell Park Memorial Institute; SDS, Sodium Dodecyl Sulfate; TAMRA, Carboxytetramethylrhodamine.; Tm, melting temperature; UV–vis, ultraviolet-visible.

* Corresponding author.
E-mail address: eva.royo@uah.es (E. Royo).

https://doi.org/10.1016/j.jinorgbio.2023.112326
Received 12 May 2023; Received in revised form 29 June 2023; Accepted 10 July 2023
Available online 13 July 2023

1. Introduction

Cancer cells need a higher level of glucose, a manifestation of the *Warburg effect* [1], an altered metabolic state in which many cancer cells can survive even under hypoxic conditions. Such an enhanced uptake for glucose depends on overexpression of glucose receptors and transporters, leading to the assumption that carbohydrate motifs could target specific proteins existing in malignant cells, and thus, open a window for the design of unconventional, relevant molecules for cancer diagnosis and therapy [2–9]. Moreover, glycans dot the surface of all cells and serve as cellular identification labels to the surrounding world, where carbohydrate-binding protein interactions are required for cell differentiation and progress of a variety of pathological states [5,10,11]. Concerning cancer diseases, such interactions are involved in cell adhesion, migration, and angiogenesis-related processes, all closely related events to metastasis [12,13]. Organic glycoconjugation is already a well-recognized strategy in the search for targeted anticancer agents, and a variety of them have been investigated and reported to have antimetastatic potential [3,14,15].

Among the vast variety of metal compounds tested as potential anticancer drugs, the enormous interest aroused by ruthenium derivatives was due to the antimetastatic properties of NAMI-A (imidazolium *trans*-[tetrachloridobis(dimethylsulfoxide)(1H-imidazole)-ruthenate(III)]) [16] and the organometallic compound of the RAPTA family [$RuCl_2(\eta^6$-p-cymene)(PTA)] (PTA = 1,3,5-triaza-7-phosphoadamantane, RAPTA-C) [17]. Soon it became evident that this unique feature was a breakthrough [18–22], and research on the metastatic profiles and related molecular mechanisms and targets of several metal compounds grew up consistently [23–25].

Many metal-glycoconjugates have been synthesized and studied [3,4,6–9]; most of the efforts have been directed so far toward the investigation of the glycoconjugation effect on cell internalization, cytotoxic selectivity and/or targeting of specific carbohydrate transport proteins [26–39]. A variety of ruthenium compounds containing glycoconjugated ligands have also been reported and recently reviewed elsewhere [7,9,31]. However, the effect that ruthenium glycoconjugates exerts on the inhibition of metastatic events occurring in malignant cells has been only barely explored [28,29,40], while it remains understudied whether the carbohydrate moiety has any role in such processes.

Bearing that in mind, we planned to prepare a new family of arene ruthenium glycoconjugates to compare their anticancer properties with that of the corresponding metal aglycone. We were especially interested in whether and how carbohydrates affect the in vitro selective cytotoxicity and the antimetastatic potential.

We report herein the synthesis and full characterization of water-soluble p-cymene Ru(II) compounds incorporating one *N*-(1,10-phenanthrolin-5-yl)-β-glycopyranosylamine as ligand. Their behaviour in physiologically relevant conditions has been investigated by ^{1}H NMR spectroscopy. The cytostatic and cytotoxic potential of the novel ruthenium glycoconjugates has been tested against human prostate cancer (PC-3) and non-tumorigenic immortalized human prostatic epithelial (RWPE-1) cells and compared with that of the corresponding metal aglycone [Ru(p-cymene)Cl{*N*-(1,10-phenanthroline-5-amine}][Cl]) (**5**), previously reported by Espino and García [41]. Cell viability has also been investigated in the presence of a glucose transporter (GLUT) inhibitor. In addition, we report the effect of the compounds on PC-3 cells migration and pro-metalloproteinases 2, 9 (proMMP-2, proMMP-9), and metalloproteinase 9 (MMP-9) activity. Evaluation of metal compounds-DNA interactions by a variety of techniques and cell cycle assay will be discussed as well.

2. Experimental section

2.1. Materials and methods

Synthesis of novel arene-ruthenium(II) complexes were performed without the exclusion of moisture or air. D(+)-Glucose, D(+)-Mannose, L(−)-Rhamnose, L(−)-Xylose, 5-amine-1,10-phenanthroline, [Ru(*p*-cymene)$Cl_2]_2$ and cisplatin (cis-[$PtCl_2(NH_3)_2$]) were purchased from Sigma-Aldrich. All reagents commercially available were used without further purification. Ruthenium aglycone [Ru(p-cymene)Cl{*N*-(1,10-phenanthroline-5-amine}][Cl]) was prepared as previously reported by Espino and Garcia [41]. Nuclear Magnetic Resonance (NMR) spectra were recorded on a Bruker 400 Ultrashield system. ^{1}H and ^{13}C chemical shifts are reported relative to tetramethylsilane. ^{15}N chemical shifts are reported relative to liquid ammonia (25 °C). Compounds concentrations used were within the range 15–25 mM. Coupling constants *J* are given in Hertz (Hz). Elemental analyses and High-Resolution Electrospray Ionization Mass Spectroscopy (HR-ESI-MS) were performed at the Universidad Autónoma de Madrid. Infrared (IR) spectra was recorded on a Fourier transform infrared (FTIR) PerkinElmer (Spectrum 2000) spectrophotometer on KBr pellets. The pH was measured in a HANNA HI208 pH meter in distilled water and water-d_2 solutions. Ultraviolet-Visible (UV–Vis) spectra were recorded at room temperature in water solutions of the compounds with a PerkinElmer Lambda 35 spectrophotometer. Compounds concentrations used were within the range 8–50 μM. Inductively Coupled Plasma Optical Emission Spectroscopy (ICP-OES) assays were performed on an *ICP-OES 20 Varian-Agilent SPS3 instrument* at *Centro de Apoyo a la Investigación en Química* (CAI), Universidad de Alcalá.

2.1.1. *N-(1,10-phenanthroline-5-yl)-β-xylopyranosylamine (**d**)*

All N-(1,10-phenanthrolin-5-yl)-β-glycopyranosylamines were prepared using the synthesis (method D) described by Duskova et al. [42]. Pale yellow powder, 86%. Anal. Calcd (%) for $C_{17}H_{17}N_3O_4$x1H_2O (345.35500): C, 59.12; H, 5.55; N, 12.17. Found: C, 58.87; H, 5.05; N, 12.24. FTIR (KBr, cm^{-1}): υ 3372 br (NH and OH), 1618 s (δ NH), 1602 s, 1556 s, 1428 s (υ C═C, υ C═N). ^{1}H NMR (plus Attached Proton Test (APT), plus gradient Heteronuclear Single Quantum Coherence (gHSQC), plus Heteronuclear Multiple Bond Correlation (HMBC), plus Correlated Spectroscopy (COSY), 400.1 MHz, 293 K DMSO-d_6): δ 9.07 (dd, 1H, J_{HH} = 4.2, 1.7 Hz, $H^{2'}$), 8.83 (dd, 1H, J_{HH} = 8.5, 1.7 Hz, $H^{4'}$), 8.76 (dd, 1H, J_{HH} = 4.3, 1.8 Hz, $H^{9'}$), 8.19 (dd, 1H, J_{HH} = 8.1, 1.8 Hz, $H^{7'}$), 7.77 (dd, 1H, J_{HH} = 8.5, 4.2 Hz, $H^{3'}$), 7.57 (dd, 1H, J_{HH} = 8.1, 4.3 Hz, $H^{8'}$), 6.99 (s, 1H, $H^{6'}$), 6.87 (d, 1H, J_{HH} = 8.0 Hz NH), 5.10 (d, 1H, J_{HH} = 4.5 Hz OH^3), 5.04[a] (d, 1H, J_{HH} = 4.3, OH^4), 5.03[a] (d, 1H, J_{HH} = 5.3, OH^2), 4.65 (app t, 1H, J_{HH} = 8.6, 8.0 Hz, H^1), 3.78 (dd, 1H, J_{HH} = 10.1, 3.9 Hz, H^{5e}), 3.51 (app td, 1H, J_{HH} = 8.6, 5.3 Hz, H^2), 3.38[b] (m, 2H, H^4, H^{5ax}), 3.30[c] (app td, J_{HH} = 8,6, 4.5, Hz, H^3); 3.40 (ddd, 1H, J_{HH} = 10.3, 8.7, 4.0 Hz, H^4), 3.37 (app t, 1H, J_{HH} = 10.3, 10.0 Hz, H^{5ax}) H^{5ax} and H^{5e} indicate the axial and equatorial protons of pyranose CH_2 group; [a]overlapped signals; [b]partially overlapped signals in DMSO-d_6-water-d_2; [c]partially overlapped with H_2O signal, H^3 signal appears at 3.31 (appt, 1H, J_{HH} = 8.7, 8.5 Hz). ^{13}C NMR (plus APT, plus HSQC, plus HMBC, 100.6 MHz, 293 K, DMSO-d_6) δ 149.9 (−, $C^{2'}$), 146.4 (+, $C^{10b'}$), 146.2 (−, $C^{9'}$), 141.5 (+, $C^{10a'}$), 140.7 (+, $C^{5'}$), 134.3 (−, $C^{7'}$), 131.1 (−, $C^{4'}$), 130.5 (+, $C^{6a'}$), 123.8 (−, $C^{8'}$), 122.6 (−, $C^{3'}$), 122.4 (+, $C^{4a'}$), 102.0 (−, $C^{6'}$), 86.2 (−, C^1, $^1J_{C1\text{-}H1}$ = 151 Hz), 77.9 (−, C^3), 72.9 (−, C^2), 70.3 (−, C^4) 67.1 (+, C^5). ^{15}N NMR (HMBC, 40.5 MHz, DMSO-d_6) δ 310.0 ($N^{1'}$), 304.5 ($N^{10'}$), 83.6 (NH).

2.1.2. *General procedure for the synthesis of arene-Ru(II) glycoconjugates (**1–4**)*

A solution of [Ru(p-cymene)$Cl_2]_2$ (60 mg, 0.098 mmol) and 0.196 mmol of the organic phenanthroline **a**·H_2O (73.5 mg, **b**·2H_2O(77.1 mg), **c**·2H_2O (73.9 mg) or **d**·2H_2O (67.7 mg) in methanol (5 mL) were stirred for 12 h at room temperature. The final solutions were filtered and dried under vacuum to afford yellow-brownish solids. Filtration is mandatory, since traces of unreacted pro-ligands could occasionally coexist with the final product. This is due to the phenanthroline glycoconjugates hygroscopicity, which difficults their accurate molecular weight determination. Yields: 123.5 mg, 0.186 mmol, 95% (**1**), 124.8 mg, 0.188 mmol,

96% (**2**), 120.5 mg, 0.186 mmol, 95% (**3**), 121.6 mg, 0.192 mmol, 98% (**4**).

2.1.3. [Ru(p-cymene)Cl{N-(1,10-phenanthrolin-5-yl)-β-glucopyranosylamine}]Cl (**1**)

Anal. Calcd (%) for $C_{28}H_{33}N_3O_5RuCl_2{\cdot}3H_2O$ (717.1158): C, 46.84; H, 5.48; N, 5.86. Found: C, 46.67; H, 4.91; N, 5.76. HR-ESI-MS *m/z* (**1**): $[M]^+$ calcd for $C_{28}H_{33}N_3O_5RuCl$ 628.1151; found: 628.1146. Solubility in H_2O at 24 °C (mM): 22.7, pH (16 mM) in H_2O at 24 °C: 6.81. FTIR (KBr, cm^{-1}): υ 3356 br (NH and OH), 1628 s (δ NH), 1603 s, 1556 s, 1466 s (υ C═C, υ C═N). ^{1}H NMR (plus HSQC, plus HMBC, plus COSY, 400.1 MHz, 293 K DMSO-d_6) As described in the Discussion paragraph, metal compounds **1**–**4** are observed in solution as a mixture of two epimers (**1**/**4–1** and **1**/**4–1′**). While the two sets of resonances are perceptible by ^{13}C NMR, the ^{1}H NMR spectra shows overlapping of most of the signals, therefore resonances multiplicity is obscured. In the following data, we describe the global integration and the apparent (app) multiplicity of the signals observed, exception made for those (OH^2, for **1** and **4**, $H^{6'}$ for **3** and **4** and $H^{7'}$ for **3**) which allow multiplicity identification and integration. δ 9.90 (br, 2H, $H^{2'}$ **1–1** + **1–1**), 9.52 (app d, 2H, $H^{9'}$ **1–1** + **1–1**), 9.41 (app d, 2H, $H^{4'}$ **1–1** + **1–1′**), 8.49 (app d, 2H, $H^{7'}$ **1–1** + **1–1′**), 8.13 (ap dd, 2H, $H^{3'}$ **1–1** + **1–1′**), 7.91 (app dd, 2H, $H^{8'}$ **1–1** + **1–1′**), 7.74 (br, 2H, NH **1–1** + **1–1′**), 7.18 (app s, 2H, $H^{6'}$ **1–1** + **1–1′**), 6.29 (app d, 4H, $H_{ar}^{(CH3)}$ **1–1** + **1–1′**), 6.06 (app t, 4H, $H_{ar}^{(i\text{-}Pr)}$ **1–1** + **1–1′**), 5.25 (d, 1H, OH^2 **1–1**), 5.20 (d, 1H, OH^2 **1–1′**), 5.11 (app d, 2H, OH^3 **1–1** + **1–1′**), 5.04 (app d, 2H, OH^4 **1–1** + **1–1′**), 4.66 (app dd, 2H, H^1 **1–1** + **1–1′**), 4.46 (app dd, 2H, OH^6 **1–1** + **1–1′**), 3.72 (m, 2H, H^6 **1–1** + **1–1′**), 3.56–3.35 (m, 8H, H^2, H^6, H^5, H^3 **1–1** + **1–1′**), 3.22 (app m, 2H, H^4, **1–1** + **1–1′**), 2.55 (overlapped with DMSO, $CH^{(i\text{-}Pr)}$ **1–1** + **1–1′**), 2.18 (s, 3H, CH_3, **1–1**), 2.19 (s, 3H, CH_3, **1–1′**), 0.86 (m, 12H, $2CH_3^{(i\text{-}Pr)}$ **1–1** + **1–1'**). ^{13}C NMR (plus APT, plus HSQC, plus HMBC, 100.6 MHz, 293 K, DMSO-d_6) **1–1** + **1–1′**: δ 155.7, 155.6 (–, $C^{2'}$), 151.3, 151.2 (–, $C^{9'}$), 145.7, 145.7 (+, $C^{10b'}$), 142.4, 142.3 (+, $C^{5'}$), 139.8, 139.7 (+, $C^{10a'}$), 135.8, 135.8 (–, $C^{7'}$), 134.2, 134.1 (–, $C^{4'}$), 131.9, 131.8 (+, $C^{6a'}$), 126.1, 126.1 (–, $C^{8'}$), 124.8, 124.8 (–, $C^{3'}$), 123.5, 123.5 (+, $C^{4a'}$), 103.4, 103.3 (+, $C_{ipso}^{(i\text{-}Pr)}$), 103.1, 103.0 (+, $C_{ipso}^{(CH3)}$), 101.1, 101.0 (–, $C^{6'}$), 86.3, 86.2, 86.0, 85.9 (–, C_6H_4), 85.0, 84.9 (–, C^1), 83.7, 83.7, 83.4, 83.4 (–, C_6H_4), 77.8, 77.8 (–, C^5), 77.4, 77.3 (–, C^3), 72.2, 72.1 (–, C^2), 70.1, 70.0 (–, C^4), 60.9, 60.8 (+, C^6), 30.3, 30.3 (–, $CH^{(i\text{-}Pr)}$), 21.6, 21.6, 21.5, 21.5 (–, $2CH_3^{(i\text{-}Pr)}$), 18.3, 18.3 (–, CH_3). ^{15}N NMR (HMBC, 40.5 MHz, DMSO-d_6) **1–1** + **1–1′**: δ 236.4 ($N^{1'}$), 233.3 ($N^{10'}$), 88.2 (NH).

2.1.4. [Ru(p-cymene)Cl{N-(1,10-phenanthrolin-5-yl)-β-mannopyranosylamine}]Cl (**2**)

Anal. Calcd (%) for $C_{28}H_{33}N_3O_5RuCl_2{\cdot}3H_2O$ (717.1158): C, 46.84; H, 5.48; N, 5.86. Found: C, 46.83; H, 4.95; N, 5.91. HR-ESI-MS *m/z* (2): $[M]^+$ calcd for $C_{28}H_{33}N_3O_5RuCl$ 628.1151; found: 628.1140. Solubility in H_2O at 24 °C (mM): 25.2. pH (16 mM) in H_2O at 24 °C: 6.83. FTIR (KBr, cm^{-1}): υ 3379 br (NH and OH), 1626 s (δ NH), 1598 s, 1503, 1466 s (υ C═C, υ C═N). ^{1}H NMR (plus HSQC, plus HMBC, plus COSY, 400.1 MHz, 293 K DMSO-d_6) δ (ppm): 9.91 (br, 2H, $H^{2'}$ **2–1** + **2–1′**), 9.55 (app d, 2H, $H^{9'}$ **2–1** + **2–1′**), 9.36 (app dd, 2H, $H^{4'}$ **2–1** + **2–1′**), 8.50 (app d, 2H, $H^{7'}$ **2–1** + **2–1′**), 8.12 (app dd, 2H, $H^{3'}$ **2–1** + **2–1′**), 7.93 (app dd, 2H, $H^{8'}$ **2–1** + **2–1′**), 7.23 (m, 4H, NH, $H^{6'}$ **2–1** + **2–1′**), 6.31 (app d, 4H, $H_{ar}^{(CH3)}$ **2–1** + **2–1′**), 6.09 (br, 4H, $H_{ar}^{(i\text{-}Pr)}$ **2–1** + **2–1′**), 5.47 (app d, 2H, OH^2 **2–1** + **2–1′**), 4.96 (app dd, 2H, H^1 **2–1** + **2–1′**), 4.88 (app d, 2H, OH^4 **2–1** + **2–1′**), 4.75 (app t, 2H, OH^3 **2–1** + **2–1′**), 4.42 (br, 2H, OH^6 **2–1** + **2–1′**), 3.97 (br, 2H, H^2 **2–1** + **2–1′**), 3.74 (m, 2H, H^6 **2–1** + **2–1′**), 3.46 (m, 6H, H^4, H^6, H3 **2–1** + **2–1′**), 3.37 (m, 2H, H^5 **2–1** + **2–1′**), 2.57 (DMSO overlapped, $CH^{(i\text{-}Pr)}$ **2–1** + **2–1′**), 2.18 (app d, 6H, CH_3 **2–1** + **2–1′**), 0.87 (m, 12H, $2CH_3^{(i\text{-}Pr)}$ **2–1** + **2–1′**). ^{13}C NMR (plus APT, plus HSQC, plus HMBC, 100.6 MHz, 293 K, DMSO-d_6) **2–1** + **2–1′**: δ 155.8, 155.7 (–, $C^{2'}$); 151.5, 151.4 (–, $C^{9'}$); 145.6, 145.6 (+, $C^{10b'}$); 141.6, 141.5 (+, $C^{5'}$); 140.0, 139.9 (+, $C^{10a'}$); 136.0, 135.9 (–, $C^{7'}$); 134.0, 133.9 (–, $C^{4'}$); 131.7, 131.6 (+, $C^{6a'}$); 126.2, 126.1 (–, $C^{8'}$); 125.0, 124.9 (–, $C^{3'}$); 123.5, 123.4 (+, $C^{4a'}$); 103.4, 103.3 (+, $C_{ipso}^{(i\text{-}Pr)}$); 103.0, 102.9 (+, $C_{ipso}^{(CH3)}$); 102.2, 102.0 (–, $C^{6'}$); 86.2, 86.2, 86.0, 85.9 (–, C_6H_4); 83.8, 83.8, 83.7, 83.5 (–, C_6H_4); 82.4, 82.3 (–, C^1); 78.3, 78.2 (–, C^5); 74.2, 74.1 (–, C^3); 70.5, 70.5 (–, C^2); 67.3, 67.2 (–, C^4); 61.3, 61.2 (+, C^6); 30.4, 30.4 (–, $CH^{(i\text{-}Pr)}$); 21.7, 21.6, 21.6, 21.5 (–, $2CH_3^{(i\text{-}Pr)}$); 18.3, 18.3 (–, CH_3). ^{15}N NMR (HMBC, 40.5 MHz, DMSO-d_6) **2–1** + **2–1′**: δ 243.4 ($N^{1'}$), 234.9 ($N^{10'}$), 86.1 (NH). Characterization in water-d_2, [Cl] = 240 mM, ^{1}H NMR (plus HSQC, plus HMBC, plus COSY, 400.1 MHz, 293 K water-d_2), ratio 1:0.5 (**2–1** + **2–1'**) δ (ppm) 2–1: 9.88 (d, J_{HH} = 5.39, 1H, $H^{2'}$), 9.50 (br, 1H, $H^{9'}$), 8.90 (d, J_{HH} = 8.85, 1H, $H^{4'}$), 8.12 (dd, J_{HH} = 8.85, J_{HH} = 5.12, 1H, $H^{3'}$), 8.00 (d, J_{HH} = 8.56, 1H, $H^{7'}$), 7.76 (dd, J_{HH} = 8.56, J_{HH} = 5.71, 1H, $H^{8'}$), 6.63 (s, 1H, $H^{6'}$), 6.20 (br, 2H, $H_{ar}^{(CH3)}$), 6.00 (br, 2H, $H_{ar}^{(i\text{-}Pr)}$), 4.27 (s, 1H, H^1), 3.92–3.57 (m 6H, H^2, $2H^6$, H^5, H^3, H^4), 2.55 (m, 1H, $CH^{(i\text{-}Pr)}$), 2.23 (app s, 3H, CH_3), 0.89 (app t, 6H, $2CH_3^{(i\text{-}Pr)}$. 2–1′: 9.74 (d, J_{HH} = 5.39, 1H, $H^{2'}$), 9.50 (br, 1H, $H^{9'}$), 8.82 (d, J_{HH} = 8.85, 1H, $H^{4'}$), 8.50 (d, J_{HH} = 8.56, 1H, $H^{7'}$), 7.92 (m, 2H, $H^{3'}$ and $H^{8'}$), 7.25 (s, 1H, $H^{6'}$), 6.20 (br, 2H, $H_{ar}(CH_3)$), 6.00 (br, 2H, $H_{ar}^{(i\text{-}Pr)}$), 5.20 (s, 1H, H^1), 4.22 (app s, 1H, H^2), 4.02 (app d, 1H, H^6), 3.92–3.57 (m 4H, H^6, H^3, H^5, H^4), 2.55 (m, 1H, $CH^{(i\text{-}Pr)}$), 2.23 (app s, 3H, CH_3), 0.93 (app t, 6H, $2CH_3^{(i\text{-}Pr)}$. ^{13}C NMR (plus APT, plus HSQC, plus HMBC, 100.6 MHz, 293 K, water-d_2), **2–1**: δ 155.5 (–, $C^{2'}$), 152.0 (–, $C^{9'}$), 146.4 (+, $C^{10b'}$), 141.2, 140.3 (+, $C^{5'}$, $C^{10a'}$); 137.3 (–, $C^{7'}$), 133.7 (–, $C^{4'}$), 132.3 (+, $C^{6a'}$), 126.8 (–, $C^{8'}$), 125.8 (–, $C^{3'}$), 124.6 (+, $C^{4a'}$), 104.3 (+, $C_{ipso}^{(i\text{-}Pr)}$), 104.1 (+, $C_{ipso}^{(CH3)}$), 103.9 (–, $C^{6'}$), 87.0, 86.8 (–, C_6H_4), 84.4, 84.1 (–, C_6H_4), 82.6 (–, C^1), 77.4 (–, C^4), 74.0 (–, C^3), 71.2 (–, C^2), 67.3 (–, C^5), 61.4 (+, C^6), 30.9 (–, $CH^{(i\text{-}Pr)}$), 21.3 (–, $2CH_3^{(i\text{-}Pr)}$), 18.5 (–, CH_3). **2–1′**: δ 155.5 (–, $C^{2'}$), 152.1 (–, $C^{9'}$), 146.4 (+, $C^{10b'}$), 141.2, 140.3 (+, $C^{5'}$, $C^{10a'}$); 136.9 (–, $C^{7'}$), 133.7 (–, $C^{4'}$), 132.3 (+, $C^{6a'}$), 126.8 (–, $C^{8'}$), 125.8 (–, $C^{3'}$), 124.6 (+, $C^{4a'}$), 104.3 (+, $C_{ipso}^{(i\text{-}Pr)}$), 104.1 (+, $C_{ipso}^{(CH3)}$), 104.0 (–, $C^{6'}$), 87.0, 86.8 (–, C_6H_4), 84.4, 84.1 (–, C_6H_4), 82.0 (–, C^1), 77.4 (–, C^4), 74.0 (–, C^3), 71.2 (–, C^2), 67.3 (–, C^5), 61.4 (+, C^6), 30.9 (–, $CH^{(i\text{-}Pr)}$), 21.3 (–, $2CH_3^{(i\text{-}Pr)}$), 18.5 (–, CH_3). ^{15}N NMR (HMBC, 40.5 MHz, water-d_2) **2–1** + **2–1′**: δ 232.0 ($N^{1'}$), 232.1 ($N^{10'}$), NH not observed.

2.1.5. [Ru(p-cymene)(OH$_2$){N-(1,10-phenanthrolin-5-yl)-β-mannopyranosylamine}][NO$_3$]$_2$ (**2·OH$_2$**)

A solution of **2** (12.2 mg, 0.018 mmol) and $AgNO_3$ (6.25 mg, 0.037 mmol) in water (2.5 mL) was stirred for 12 h at room temperature. The final suspension was filtered to eliminate solid AgCl, and the solvent was evaporated to afford a brown solid. Yield: 12.9 mg (98%). HR-ESI-MS *m/z* (**2·OH$_2$**): $[M\text{-}H_2O]^{2+}$ calcd for $C_{28}H_{33}N_3O_5Ru$ 296.5730; found: 296.5721 (100%), $[M]^{2+}$ calcd for $C_{28}H_{35}N_3O_6Ru$ 305.5783; found: 296.5777 (35%), $[M^{2+}\text{-}H_2O\text{-}H^+]^+$ calcd for $C_{28}H_{32}N_3O_5Ru$ 592.1388; found: 592.1379 (34%). ^{1}H NMR (plus HSQC, plus HMBC, plus COSY, 400.1 MHz, 293 K water-d_2) δ (ppm): 10.00 (br, 2H, H2' **2·OH$_2$–1** + **2·OH$_2$–1′**), 9.68 (app d, 2H, $H^{9'}$ **2·OH$_2$–1** + **2·OH$_2$–1′**), 9.06 (app dd, 2H, $H^{4'}$ **2·OH$_2$–1** + **2·OH$_2$–1′**), 8.60 (app d, 2H, $H^{7'}$ **2·OH$_2$–1** + **2·OH$_2$–1′**), 8.16 (app dd, 2H, $H^{3'}$ **2·OH$_2$–1** + **2·OH$_2$–1′**), 7.99 (app dd, 2H, $H^{8'}$ **2·OH$_2$–1** + **2·OH$_2$–1′**), 7.33 (app s, 2H, $H^{6'}$ **2·OH$_2$–1** + **2·OH$_2$–1′**), 6.38 (br, 4H, $H_{ar}^{(CH3)}$ **2·OH$_2$–1** + **2·OH$_2$–1′**), 6.16 (br, 4H, $H_{ar}^{(i\text{-}Pr)}$ **2·OH$_2$–1** + **2·OH$_2$–1′**), 5.32 (app d, 2H, H^1 **2·OH$_2$–1** + **2·OH$_2$–1′**), 4.27 (app dd, 2H, H^2 **2·OH$_2$–1** + **2·OH$_2$–1′**), 4.00 (br, 2H, H^6 **2·OH$_2$–1** + **2·OH$_2$–1′**), 3.87–3.72 (m, 8H, H^3, H^5, H^6, H^4 **2·OH$_2$–1** + **2·OH$_2$–1′**), 3.37, 2.51 (m, 2H, $CH^{(i\text{-}Pr)}$ **2·OH$_2$–1** + **2·OH$_2$–1′**), 2.23 (app s, 6H, CH_3 **2·OH$_2$–1** + **2·OH$_2$–1′**), 0.90 (app dd, 12H, $2CH_3^{(i\text{-}Pr)}$ **2·OH$_2$–1** + **2·OH$_2$–1'**). ^{13}C NMR (plus APT, plus HSQC, plus HMBC, 100.6 MHz, 293 K, water-d_2) **2·OH$_2$–1** + **2·OH$_2$–1′**: δ 155.3, 155.5 (–, $C^{2'}$); 151.8, 151.8 (–, $C^{9'}$), 146.5, 146.4 (+, $C^{10b'}$); 141.2, 141.2 (+, $C^{10a'}$); 140.5, 140.5 (+, $C^{5'}$); 137.8, 137.8 (–, $C^{7'}$); 134.4, 134.3 (–, $C^{4'}$); 131.9, 131.8 (+, $C^{6a'}$); 126.4, 126.4 (–, $C^{8'}$); 125.4, 125.4 (–, $C^{3'}$); 124.3, 124.2 (+, $C^{4a'}$); 103.7, 103.7 (+, $C_{ipso}^{(i\text{-}Pr)}$); 103.6, 103.5 (+, $C^{6'}$); 100.5, 100.5 (–, $C_{ipso}^{(CH3)}$); 86.6, 86.6, 86.4, 86.3 (–, C_6H_4); 83.1, 83.0, 82.8, 82.8 (–, C_6H_4); 82.0, 82.0 (–, C^1); 79.9, 79.9 (–, C^4); 73.4, 73.4 (–, C^3); 70.7, 70.7 (–, C^2); 66.7, 66.7 (–, C^5); 60.8, 60.8 (+, C^6); 30.1, 30.1 (–, $CH^{(i\text{-}Pr)}$); 20.6, 20.6, 20.6, 20.6 (–, $2CH_3^{(i\text{-}Pr)}$); 17.3, 17.3 (–, CH_3). ^{15}N NMR (HMBC, 40.5 MHz, DMSO-d_6) **2·OH$_2$–1** + **2·OH$_2$–1′**: δ 227.4 ($N^{1'}$), 224.2 ($N^{10'}$), 78.21 (NH).

2.1.6. [Ru(p-cymene)Cl{N-(1,10-phenanthrolin-5-yl)-β-rhamnopyranosylamine}]Cl (3)

Anal. Calcd (%) for $C_{28}H_{33}N_3O_4RuCl_2{\cdot}2H_2O$ (683.1103): C, 49.20; H, 5.46; N, 6.15. Found: C, 49.51; H, 5.32; N, 6.21. HR-ESI-MS *m/z*: $[M]^+$ calcd for $C_{28}H_{33}N_3O_5RuCl$ 612.1202; found: 612.1177. Solubility in H_2O at 24 °C (mM): 22.5. The value of pH (16 mM) in H_2O at 24 °C: 7.17. FTIR (KBr, cm^{-1}): υ 3379 br (NH and OH), 1626 s (δ NH), 1598 s, 1503, 1466 s (υ C═C, υ C═N). ^{1}H NMR (plus HSQC, plus HMBC, plus COSY, 400.1 MHz, 293 K DMSO-d_6) δ (ppm) diastereomer ratio 1:0.7: 9.91 (app d, 2H, $H^{2'}$ **3–1** + **3–1′**), 9.55 (m, 4H, $H^{9'}$ and H4′ **3–1** + **3–1′**), 8.58 (d, 1H, $H^{7'}$ **3–1′**), 8.55 (d, 1H, $H^{7'}$ **3–1**), 8.09 (m, 2H, $H^{3'}$ **3–1** + **3–1′**), 7.89 (m, 2H, $H^{8'}$ **3–1** + **3–1′**), 7.38 (2d, 2H, NH **3–1** + **3–1′**) 7.16 and 7.12 (2 s, 2H, $H^{6'}$ **3–1** + **3–1′**), 6.30 (app d, 4H, $H_{ar}^{(CH3)}$ **3–1** + **3–1′**), 6.06 (m, 4H, $H_{ar}^{(i\text{-}Pr)}$ **3–1** + **3–1′**), 5.71 (br, 2H, OH^2 **3–1** + **3–1′**), 4.90 (m, 4H, H^1 and OH^4 **3–1** + **3–1′**), 4.71 (br, 2H, OH^3 **3–1** + **3–1′**), 4.00 (br, 2H, H^2 **3–1** + **3–1′**), 3.44 (br, 4H, H^3 and H^5 **3–1** + **3–1′**), 3.24 (m, 2H, H^4 **3–1** + **3–1′**), 2.56 (DMSO overlapped, $CH^{(i\text{-}Pr)}$ **3–1** + **3–1′**), 2.17 (app s, 6H, CH_3 **3–1** + **3–1′**), 1,18 (2d, 6H, $CH_3^{6'}$ **3–1** + **3–1′**), 0.85 (m, 12H, $2CH_3^{(i\text{-}Pr)}$ **3–1** + **3–1′**). ^{13}C NMR (plus APT, plus HSQC, plus HMBC, 100.6 MHz, 293 K, DMSO-d_6) **3–1** + **3–1′**: δ 155.7, 155.7 (–, $C^{2'}$), 151.5, 151.4 (–, $C^{9'}$); 146.7, 147.6 (+, $C^{10b'}$); 141.6, 141.5 (+, $C^{5'}$); 139.9, 139.9 (+, $C^{10a'}$); 136.0, 135.9 (–, $C^{7'}$); 134.0, 134.0 (–, $C^{4'}$); 131.7, 131.6 (+, $C^{6a'}$); 126.1, 126.0 (–, $C^{8'}$); 124.9, 124.8 (–, $C^{3'}$); 123.5, 123.4 (+, $C^{4a'}$); 103.5, 103.4 (+, $C_{ipso}^{(i\text{-}Pr)}$); 102.9, 102.8 (+, $C_{ipso}^{(CH3)}$); 101.5, 101.4 (–, $C^{6'}$); 86.2, 86.2, 86.0, 85.9 (–, C_6H_4); 83.8, 83.7, 83.5, 83.5 (–, C_6H_4); 82.1, 82.0 (–, C^1); 73.9, 73.8 (–, C^3); 72.9, 72.9 (–, C^5); 72.1, 72.1 (–, C^4); 70.6, 70.6 (–, C^2); 30.3, 30.3 (–, $CH^{(i\text{-}Pr)}$); 21.6, 21.6, 21.5, 21.5 (–, $CH_3^{(i\text{-}Pr)}$); 18.3, 18.2 (–, CH_3^5), 18.1, 18.0 (–, CH_3). ^{15}N NMR. (HMBC, 40.5 MHz, DMSO-d_6) **3–1** + **3–1′**: 237.1 ($N^{1'}$), 234.1 ($N^{10'}$), 81.3 (NH).

2.1.7. [Ru(p-cymene)Cl(N-(1,10-phenanthrolin-5-yl)-β-xylopyranosylamine)]Cl (4)

Anal. Calcd (%) for $C_{27}H_{31}N_3O_4RuCl_2x2H_2O$ (669.0946): C, 48.43; H, 5.27; N, 6.28. Found: C, 48.90; H, 5.22; N, 6.38. HR-ESI-MS *m/z*: $[M]^+$ calcd for $C_{27}H_{33}N_3O_4RuCl$ 598.1056; found: 598.1032. Solubility in H_2O at 24 °C (mM): 39.2. The value of pH (16 mM) in H_2O at 24 °C: 7.23. FTIR (KBr, cm^{-1}): υ 3378 br (NH and OH), 1627 s (δ NH), 1599 s, 1541 s, 1466 s (υ C═C, υ C═N). ^{1}H NMR. (plus HSQC, plus HMBC, plus COSY, 400.1 MHz, 293 K DMSO-d_6): δ 9.91 (br, 2H, $H^{2'}$ **4–1** + **4–1′**), 9.52 (app d, 2H, $H^{9'}$ **4–1** + **4–1′**), 9.43 (2d, 2H, $H^{4'}$ **4–1** + **4–1′**), 8.55 (2d, 2H, $H^{7'}$ **4–1** + **4–1′**), 8.13 (2dd, 2H, $H^{3'}$ **4–1** + **4–1′**), 7.91 (app dd, 2H, $H^{8'}$ **4–1** + **4–1′**), 7.73 (app t, 2H, NH **4–1** + **4–1′**), 7.18 (s, 1H, H6′ 4–1), 7.17 (s, 1H, $H^{6'}$ **4–1′**), 6.29 (br, 4H, $H_{ar}^{(CH3)}$ **4–1** + **4–1′**), 6.06 (m, 4H, $H_{ar}^{(i\text{-}Pr)}$ **4–1** + **4–1′**), 5.36 (d, 1H, OH^2 **4–1**), 5.30 (d, 1H, OH^2 **4–1′**), 5.17 (app d, 2H, OH^3 **4–1** + **4–1′**), 5.11 (app d, 2H, OH^4 **4–1** + **4–1′**), 4.62 (app q, 2H, H^1 **4–1** + **4–1′**), 3.75 (app d, 2H, H^5 **4–1** + **4–1′**), 3.56 (m, 2H, H^2 **4–1** + **4–1′**), 3.39 (m, 4H, H^4, $H^{5'}$ **4–1** + **4–1′**), 3.28 (m, 2H, H^3 **4–1** + **4–1′**), 2.55 (m, 2H, DMSO overlapped, CH(*i*-Pr) 4–1 + 4–1′), 2.18 (s, 3H, CH_3 **4–1**), 2.17 (s, 3H, CH_3 **4–1′**), 0.86 (m, 12H, $2CH_3^{(i\text{-}Pr)}$ **4–1** + **4–1′**). ^{13}C NMR (plus APT, plus HSQC, plus HMBC, 100.6 MHz, 293 K, DMSO-d_6) **4–1** + **4–1′**: δ 155.7, 155.7 (–, $C^{2'}$); 151.3, 151.2 (–, $C^{9'}$); 145.8, 145.7 (+, $C^{10b'}$); 142.3, 142.2 (+, $C^{5'}$); 139.8, 139.8 (+, $C^{10a'}$); 135.8, 135.8 (–, $C^{7'}$); 134.2, 134.1 (–, $C^{4'}$); 131.8, 131.7 (+, $C^{6a'}$); 126.2, 126.1 (–, $C^{8'}$); 124.9, 124.8 (–, $C^{3'}$); 123.5, 123.4 (+, $C^{4a'}$); 103.4, 103.4 (+, $C_{ipso}^{(i\text{-}Pr)}$); 103.0, 102.9 (+, $C_{ipso}^{(CH3)}$); 100.7, 100.6 (–, $C^{6'}$); 86.2, 86.1, 86.0, 85.9 (–, C_6H_4); 85.7, 85.6 (–, C^1); 83.8, 83.7, 83.5, 83.5 (–, C_6H_4); 77.3, 77.2 (–, C^3); 72.0, 71.9 (–, C^2); 69.8, 69.7 (–, C^4); 66.9, 66.8 (+, C^5); 30.4, 30.4 (–, $CH^{(i\text{-}Pr)}$); 21.7, 21.6, 21.6, 21.5 (–, $CH_3^{(i\text{-}Pr)}$); 18.3, 18.3 (–, CH_3). ^{15}N NMR (HMBC, 40.5 MHz, DMSO-d_6) **4–1** + **4–1′**: δ 244.0 ($N^{1'}$), 233.3 ($N^{10'}$), 88.9 (NH).

2.1.8. ^{1}H NMR experiments in water-d_2 at physiological pH

Phosphate buffer saline (PBS) was prepared according to Cold Spring Harbor Protocols (http://cshprotocols.cshlp.org/content/2006/1/pdb.rec8247) using NaCl, KCl, Na_2HPO_4 and $KHPO_4$ in water-d_2. Adjustment of pD (pD = pH* + 0.4, where pH* = pHmeter reading in water-d_2) was carried out using a solution of DCl (0.01 M) or NaOD (0.01 M) in water-d_2, with the help of a HANNA HI208 pHmeter. Ruthenium compounds were then dissolved in 2000 μL of the freshly prepared PBS, final pD measured (7.30–7.38) and time-dependent ^{1}HNMR spectra of 500 μL aliquots of final solutions were carried out at 25 °C. Alternatively, ruthenium compounds were dissolved in water-d_2 and adjusting pD using a solution of DCl (0.01 M) to study complexes behaviour in acidic aqueous solutions.

2.2. Metal compound-DNA interaction studies

2.2.1. Fluorescence resonance energy transfer (FRET) melting assays

A quantitative PCR kit ABI PRISM® 7000 Sequence Detection System (Applied Biosystems) was employed, in a 96-well plate format (96-Well Optical MicroAmp® Reaction Plate, Applied Biosystems, Life Technologies Corporation). The duplex deoxyribonucleic acid (dsDNA) oligonucleotide sequence, F10T (5'-FAM- TAT AGC TA TA /sp18/ TA TA GCT ATA-TAMRA-3′), was acquired to Integrated DNA Technologies (IDT), High Performance Liquid Chromatography (HPLC) purified and desalted. FAM is 6-carboxyfluorescein and TAMRA is carboxytetramethylrhodamine. As a buffering system containing chloride ions, 10 mM sodium cacodylate, 100 mM LiCl, (pH = 7.3), was used. The experiments were additionally run in the absence of chloride salts, in 10 mM phosphate buffer (NaH_2PO_4/Na_2HPO_4) pH = 7.2.

First, the duplex-forming oligonucleotide F10T was dissolved in water (Biotechnology Performance Certified, BPC grade) and a 50 μM stock solution was prepared, and then diluted to 0.5 μM and mixed with the working buffer (2×) and water (BPC grade). The DNA solution was heated at 90 °C for 10 min, cooled down slowly for 3 h and left at 4 °C overnight. Metal complexes **1**–**5** were dissolved in water and approximately 1 mM stock solutions were prepared. Stock solutions were then diluted with buffer to obtain 50 μM solutions of each compound. In a 96-well microplate, DNA solutions were mixed with solutions of tested compound and buffer to reach a total volume of 50 μL with a F10T concentration of 0.2 μM, and a compound concentration ranging between 1 and 10 μM.

The melting protocol consisted of an incubation for 5 min at 24 °C, followed by a temperature ramp with a heating rate of 1 °C/min. Conversely, the reverse folding process consisted of incubation at 96 °C for 5 min, followed by a temperature ramp with a cooling rate of −1 °C/min. Fluorescence values corresponding to the fluorophore FAM at wavelength of 516 nm (after excitation at 492 nm) were collected at each degree of temperature. Afterwards, the fluorescence data were normalized, plotted against temperature (°C) at each compound concentration, and melting temperatures (Tm) values were estimated as $T_{1/2}$.

2.2.2. Viscosity titrations

Calf Thymus (CT) dsDNA, (activated, Type XV) was purchased from Sigma Aldrich and used as provided. 10 mM phosphate buffer (NaH_2PO_4/Na_2HPO_4) pH = 7.2 was used. The viscosity measurements were performed in a Visco System AVS 470 at 25.00 ± 0.01 °C, using a microUbbelohde (K = 0.01) capillary viscometer. 6 mL of DNA solution (0.3–0.4 mM in nucleotides) in phosphate buffer were equilibrated for 20 min at 25.00 °C and then 20 flow times were registered. Small aliquots (droplets) of buffered concentrated solutions of metal complexes 1–5 (typically 1.5–2.0 mM) were added to the DNA solution. Before each flow time registration, the solutions were mixed and allowed to equilibrate for 20 min to 25.00 °C and then 20 flow times were measured. With the averaged time of the different flow time measurements and the viscometer constant, the viscosities (μ) for each point were calculated. The viscosity results were plotted as $(\mu/\mu_0)^{1/3}$, where μ_0 is the DNA solution viscosity in the absence of the ligand, versus r, the [ligand]/[DNA] ratio.

2.2.3. Equilibrium dialysis

NaH_2PO_4/Na_2HPO_4 buffer (10 mM, pH = 7.2) was used, in the same conditions as required in viscosity assays and in chloride-free FRET assays. For each dialysis assay, a 0.2 mL volume of CT dsDNA in buffer (75 μM in base pairs) was pipetted into individual dialysis units (Biotech Regenerated Cellulose (RC) membrane, part number 133192, Spectrum Laboratories, Inc.). The dialysis units were then placed in a beaker containing ca. 200 mL of a 4–5 μM solution of compound in buffer. The beaker was covered with parafilm and wrapped in aluminium foil, and its contents were allowed to equilibrate with continuous stirring for 24 h at room temperature (22 °C). At the end of the equilibration period, the DNA solutions inside the dialysis units were carefully transferred into microcentrifuge tubes and a 10.0% (*w/v*) stock solution of Sodium Dodecyl Sulfate (SDS) was added to give a final concentration of 1.0% (w/v). These solutions were allowed to equilibrate for another 2 h, after which the total concentration of the ligand (C_t) was determined by UV–vis absorbance measurements using the determined extinction coefficient for metal complexes 1–5 in the presence of 1.0% detergent. The concentration of free compound (C_f) was also determined spectrophotometrically using an aliquot of their dialysate solution. The amount of DNA-bound compound (C_b) was then calculated by the difference $C_b = C_t - C_f$ and apparent association constants (K_{app}) determined.

2.3. In vitro cell studies

2.3.1. Cell culture

The androgen-independent PC-3 and non-tumorigenic RWPE-1 cell lines were obtained from the American Type Culture Collection (Manassas, VA). RWPE-1 cells were maintained in complete keratinocyte serum-free medium supplemented with 1% penicillin/streptomycin/amphoterycin B, 50 μg/mL of bovine pituitary extract and 5 ng/mL epidermal growth factor (Life Technologies, Barcelona, Spain), PC-3 cells were maintained in RPMI-1640 (Roswell Park Memorial Institute) supplemented with 5% fetal bovine serum (FBS), 200 U/mL penicillin, 100 μg/mL streptomycin and 2 mM L-glutamine (all from Sigma-Aldrich). The culture was performed in a humidified 5% CO_2 environment at 37.00 °C. After the cells reached 70–80% confluence, they were washed with PBS, detached with 0.25% trypsin/0.2% EDTA and seeded at 5000–15000 cells per cm^2. The culture medium was changed every 2 days. Cultures were maintained under a humidified atmosphere of 95% air: 5% CO_2 at 37.00 °C. Adherent cells were allowed to attach for 24 h prior to the addition of compounds.

2.3.2. Cell viability assays

For toxicity assays, cells were seeded in flat-bottom 96-well plates ($1{\cdot}10^4$–$2.5{\cdot}10^4$ cells per well) in complete medium. Adherent cells were allowed to attach for 24 h prior to the addition of the tested compounds. Stock solutions of the compounds were freshly dissolved in the corresponding medium and then diluted in complete medium and used for sequential dilutions to desired concentrations. Control groups of untreated cells (negative control) and cisplatin treated cells (positive control) were included in the assays. Compounds were added at different concentrations and cells were incubated for 24 and 72 h for PC-3 cells and 72 h for RWPE-1 cells. Cell proliferation was determined by the MTT-reduction method. Briefly, [3-(4,5-dimethylthiazol-2-yl)-2,5-diphenyltetrazolium bromide] (MTT) (5 mg/mL in PBS) was added, and the plates were incubated for 1.5–2 h at 37.00 °C. After that time, the culture medium was removed, and the purple formazan crystals were dissolved in DMSO. The optical density was measured at 570 nm and calculated from the absorbance of untreated control cells. The IC_{50} values are presented as a mean ± S.E.M of at least three independent experiments, each comprising eight microcultures per concentration level.

2.3.3. Clonogenic assays

PC-3 cells were seeded in 6 well-plate at a density of 100 cells per well in complete media (10% FBS and 1% penicillin/streptomycin/amphotericin B). After 24 h, the culture media was removed, and the cells were treated with the metal compounds for 24 h at different concentrations. The medium was replaced every 48 h for 2 weeks. Finally, the culture media was removed, and the cells were attached with methanol/acetic acid (3:1) for 30 min, washed with PBS and dyed for 4 h with a solution 0.5% of crystal violet in water/methanol (4:1). The colony formation was quantified by measuring optical density after dissolving formed crystals in methanol. Control samples (in the absence of metal compounds) were averaged and assigned a value of 100%.

2.3.4. GLUTs inhibition study

PC-3 cells were seeded in flat-bottom 96-well plates (15,000 cells per well) in complete medium. Cells were allowed to attach for 24 h prior to the addition of the tested compounds and GLUT inhibitor (BAY-876). Stock solutions of new compounds and BAY-876 were freshly dissolved in the corresponding medium and then diluted to achieve the desire concentrations. Control groups were included in the assays. First, cells were treated with BAY-876 for 20 min at 2 (inhibition $IC_{50,}$ [43]) or 10 nM. Then, compounds were added at the desired concentrations. Cells were incubated with compounds and BAY-876 for 72 h and cell proliferation was determined by the MTT-reduction method described above.

2.3.5. Cellular uptake

For cellular uptake studies, PC-3 were seeded in a P100 plate at a density of 10^6 cells per plate in complete media (10% FBS and 1% penicillin/streptomycin/amphotericin B), and then left to attached for 24 h. The different plates were treated at the required concentrations of compounds **2**–**5** and GLUTi, when required. Cells were incubated for further 24 h, culture media was recovered (to include the ruthenium content of death cells in the analysis), and cells were washed with iced-PBS (2x3mL), detached with 3 mL of 0.25% trypsin/0.2% EDTA, and collected with their culture media. Then, samples were centrifuged 4 min at 1500 rpm and supernatant was removed to eliminate non-internalized ruthenium, culture media and trypsin. Pellets were re-suspended in 5 mL of iced-PBS.

2.3.6. ICP-OES

2 mL of each sample were processed by an oxidative acid digestion with 6 mL of 69% nitric acid (ppb trace) using high temperature and pressure, under a microwave-assisted process. The samples are diluted to 25 mL and processed in an ICP-OES *20 Varian-Agilent SPS3 instrument.* Ruthenium was quantified at 240.272 nm by interpolation into a linear calibration plot obtained with an external standard ($RuCl_3$, analysis grade).

2.3.7. Wound-healing assay

PC-3 cells were seeded in 24-well plates at a density of 90,000 cells per well in complete media (10% FBS and 1% penicillin/streptomycin/amphotericin B), and then growth to confluence for 72 h. A small wound area was made with a scraper in either the absence or presence of the complexes. Four representative fields of each wound were captured using a Nikon Diaphot 300 inverted microscope at different times (0 and 24 h). The wound areas of samples at time 0 h were averaged and assigned a value of 100%. The width of the scratch was measured with a single perpendicular line to the stretch of each wound at 0 and 24 h. Four different wounds for each complex were performed in each experiment, and at least five independent experiments were carried out.

2.3.8. Gelatin zymography

PC-3 cells were seeded in 6 well-plate at a density of $1.5{\cdot}10^4$ cells per well in complete media (10% FBS and 1% penicillin/streptomycin/amphotericin B). After 24 h, the culture media was removed, and the cells were incubated with the new compounds at different concentrations for 24 h. Then, the supernatant was collected. The samples were analyzed by a zymographic technique performing 10% SDS–PAGE with

0.1% (*w/v*) gelatin (Sigma) as the substrate. Each lane was loaded with a total protein concentration of 3 μg and subjected to electrophoresis. Gels were washed twice in 50 mM Tris (pH 7.4) containing 2.5% (*v*/v) Triton X-100 for 1 h, followed by two 10-min rinses in 50 mM Tris (pH 7.4). After SDS removal, the gels were incubated overnight in 50 mM Tris (pH 7.5) containing.

10 mM $CaCl_2$, 0.15 M NaCl, 0.1% (v/v) Triton X-100, and 0.02% sodium azide at 37 °C under constant gentle shaking. After incubation, the gels were stained with 0.25% Coomasie brilliant blue R-250 (Sigma) and destained in 7.5% acetic acid with 20% methanol. The activity of proMMP-2, proMMP-9 and MMP-9 was semiquantitatively determined by densitometry.

2.3.9. Data analysis

Results were subjected to computer-assisted statistical analysis using One- of Variance ANOVA, and differences were determined by Bonferroni's multiple comparison test. Results obtained of all biological assays were analyzed with the GraphPad Prism 8 program. Data are shown as the means of individual experiments and presented as the mean ± S.E.M (standard error of the mean). Differences of $P < 0.05$ were considered significantly different from the controls.

3. Results and discussion

3.1. Synthesis and characterization of metal compounds

The stereoselective *N*-glycosylation of 5-amino-1,10-phenanthroline with D-glucose, D-mannose and L-rhamnose was already published to afford *N*-(1,10-phenanthrolin-5-yl)-β-glycopyranosylamines (Fig.1, glycopyranosyl = D-glucopiranosyl (Glcp, **a**), D-mannopiranosyl (Manp, **b**), L-rhamnopiranosyl (Rhap, **c**)) [42]. We have used the same protocol for the synthesis of derivative *N*-(1,10-phenanthrolin-5-yl)-β-xylopyranosylamine (Xylp, **d**), which has been fully characterized by CHN elemental analysis, IR, ^{1}H, ^{13}C and ^{15}N NMR spectroscopy (Figs. S1-S7, SI).

Reaction of $[Ru(p\text{-}\eta^6\text{-cymene})Cl(\mu\text{-}Cl)]_2$ with organic derivatives **a-d** leads to new chiral-at-metal ruthenium(II) cationic compounds [Ru(p-η^6-cymene)Cl{(*N*-(1,10-phenanthrolin-5-yl)-β-glycopyranosylamine)}]Cl (where glycopyranosyl = Glcp (**1**), Manp (**2**), Rhap (**3**), Xylp (**4**)) (Fig. 2) in excellent yields (95–98%). Decomposition, hydrolysis and/or anomerization of the starting *N*-β-glycopyranosylamine were not detected. The NMR spectra of p-cymene Ru(II) glycoconjugates **1**–**4** provide conclusive evidence that the carbohydrate units retain the *N*-β-glycopyranoside structure of the pro-ligands and allow to rule out a dynamic solution equilibrium between both α and β anomers.

Since the synthetic reaction proceeds with formation of a new chiral centre at the Ru atom and carbohydrates contain fixed absolute configurations, two different diastereoisomers (epimers), distinguishable by NMR, can form. While a mixture of two analogous sets of resonances of similar intensity can be distinguished in the ^{13}C NMR spectra of compounds **1**–**4** in DMSO-d_6, overlapping of most of the ^{1}H NMR signals due to each epimer difficult an accurate determination of the epimeric ratios, especially for derivative **2**. For compounds **1**, **3** and **4**, however, some resonances due to each epimer do not overlap and allow integration, which renders epimeric ratios of ca. 1:1 (**1** or **4**) or 1:0.7 (**3**) in the mixture (see experimental section and Figs. S8, S19, S22, SI). Further epimerization [44–46] or change in the relative intensity of each set of resonances was not observed in DMSO-d_6 within the next 72 h and the temperature range of 20–60 °C (Fig. S14, SI). We also investigated whether the chloro ligand remains bound to ruthenium in DMSO-d_6 solutions, by comparison of the spectra of **1** in the absence or presence of $AgNO_3$ (Fig. S15, SI). The results indicate that the species present in DMSO-d_6 solution differs from the one formed after $AgNO_3$ addition, and points to preservation of the Ru—Cl bond in the coordinating solvent. In addition, CHN elemental analysis of the samples endorse the proposed chemical composition for derivatives **1**–**4**.

Coordination of the phenanthroline moiety as a bidentate ligand is confirmed by the changes on the NMR spectra of the metal conjugates relative to those of pro-ligands. The resonances due to H or C atoms closest to the metal change the most. Thus, ^{1}H and ^{13}C NMR signals assigned to $H^{2'}$, $H^{9'}$ and $C^{2'}$, $C^{9'}$ (see Fig.1 for numbering) are downfield shifted in the NMR spectra of compounds **1**–**4** (resonances found within the range δ 9.90–9.94 $H^{2'}$, 9.55–9.62 $H^{9'}$, 155.8–155.6 $C^{2'}$, 151.2–151.9 $C^{9'}$) relative to those assigned to the same atoms in metal free glycoconjugates **a-d** (resonances found within the range δ 9.05–9.08 $H^{2'}$, 8.74–8.76 $H^{9'}$ and 148.9–149.9 $C^{2'}$, 145.2–145.4 $C^{9'}$).

The difference between the chemical shifts of the nitrogen signals due to the phenanthroline N atoms of **a-d** (resonances within the ranges δ 312.4–311.6 $N^{1'}$, 311.6–305.5 $N^{10'}$) and metal compounds **1**–**4** (resonances within the ranges δ 236.4–244.0 $N^{1'}$, 233.3–234.9 $N^{10'}$) ratifies the proposed coordination in the final metal compounds.

Regarding IR spectra, C═N stretching frequencies are assigned to absorptions observed at υ 1556–1428 cm^{-1} in compounds **1**–**4**. These bands are shifted to lower wave numbers relative to those detected in the IR spectra of **a-d** (υ 1628–1466 cm^{-1}), as result of phenanthroline N coordination. In addition, a strong, broad band within the range 3378–3329 cm^{-1} confirms the presence of carbohydrate OH groups in free ligands as well as in metal compounds.

3.2. Behaviour of Ru(II) compounds *1*–*4* under physiological conditions

Since buffered water solutions were used in our biological studies, we decided to evaluate the pH- and time-dependent stability of novel ruthenium compounds in water-d_2 or deuterated PBS (phosphate buffer saline) by ^{1}H NMR. Freshly prepared water-d_2 solutions of compounds **1**–**4** exhibit a pH within the 6.8–7.2 interval (compound concentration

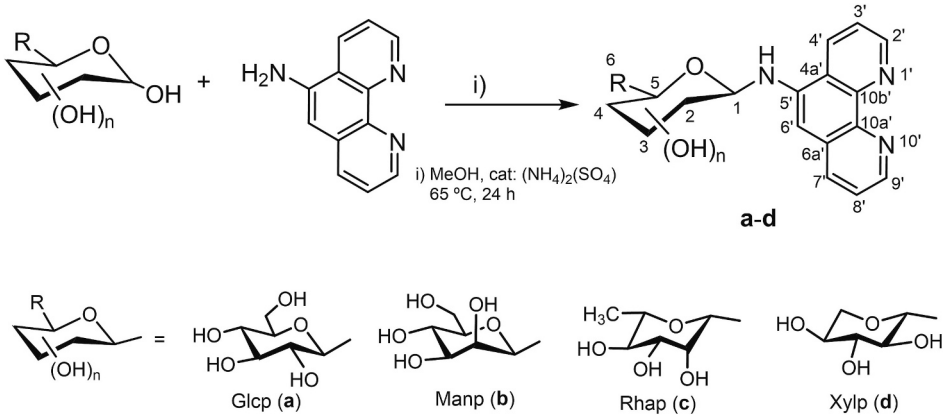

Fig. 1. Synthesis of *N*-(1,10-phenanthrolin-5-yl)-β-glycopyranosylamine pro-ligands, **a**-**d**.

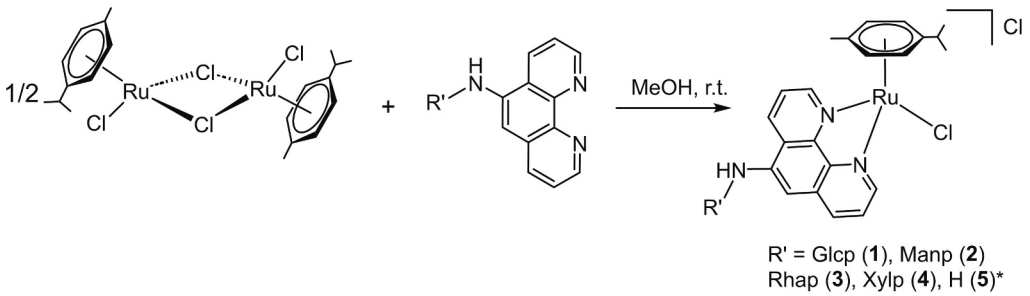

Fig. 2. Synthesis of novel p-cymene Ru(II) glycoconjugates **1**–**4** and *Espino and García compound **5** [41].

ca. 16 mM). Right after dissolution in water-d_2, the ^{1}H NMR spectra show, together with a major set of resonances assigned to the two expected epimers, a minor group of signals slightly shifted downfield. An example of the spectra recorded for **1** in water-d_2 is shown in Fig. 3(A). These firstly observed sets of resonances do not change within the next 72 h in a pH range 3.0–7.4 (Figs. S25, S26, SI).

In contrast, the spectra recorded in deuterated PBS ([NaCl] = 137 mM, pH* = 7.4 where pH* = pH meter reading in water-d_2, Fig. 3(B), or after addition of NaCl at concentrations >100 mM, (Fig. 3(C), (D)) to the water-d_2 solutions of the compounds, exhibit only signals that are coincident with the major set of resonances observed in pure water-d_2. These resonances can be unequivocally assigned to $[Ru\text{-}Cl]^+$ species (Figs. S29-S33, SI), according with the proposed equilibrium displayed in Fig. 4, where the increase of $[Cl^-]$ disfavor the aquation process and render species $[Ru\text{-}Cl]^+$. This observed experimental behaviour allow us to conclude that aquation should be precluded in the bloodstream, ($[Cl^-] \approx 100$ mM, Fig. 3(B)), but could happen in some extent in the cytoplasm ($[Cl^-] \approx 4$–10 mM, Fig. 3(C)) [47].

In saline water-d_2, the ratio of epimers of compounds **1**–**4** can be calculated by ^{1}H NMR resonances integration (Figs. S27, S28, SI). Right after dilution in saline (or PBS) water-d_2, compounds **1** and **4** are observed as a 1:1 mixture of epimers, whose integrals remain unchanged after 72 h at 40 °C. In contrast, for derivatives **2** and **3** epimerization proceeds from an initial equimolar mixture to a final ratio of ca. 1:0.5 after the first 48 h (Fig. S28, SI). Additionally, HR-ESI-MS of the samples obtained show molecular peaks with the correct isotopic pattern for $[M]^+$, and evidence the presence of the Ru-chloro bond in these novel compounds, under the conditions used (Figs. S39-S42).

The nature of the minor resonances firstly detected in water-d_2

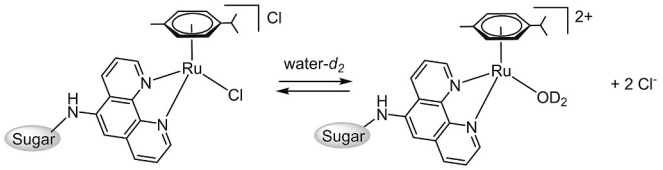

Fig. 4. Aqua-complex formation equilibrium.

(Fig. 3A) was investigated by addition of $AgNO_3$ to the deuterated water solutions of the compounds, which resulted in precipitation of AgCl and exhibition of a set of resonances matching only the minor signals observed in pure water-d_2, and assignable to $[Ru(OD_2)]^{2+}$ species (Fig. 3 (E)).

The aqua derivative [Ru(p-cymene)(OH_2){*N*-(1,10-phenanthroline-5-yl)-β-D(+)-mannopyranosylamine}][NO_3]$_2$ (**2·OH$_2$**), could be fully characterized by NMR as a mixture of two epimers (see Experimental part and Figs. S34-S38, SI). Their integration was prevented due to overlapping of all the ^{1}H NMR resonances in water-d_2, but two sets of resonances of similar intensity became evident in the ^{13}C NMR spectrum (Fig. S35b, SI). HR-ESI-MS of **2·OH$_2$** shows the molecular peak with the correct isotopic pattern for $[M]^{2+}$ at m/z = 305.5777 (35%), and $[M\text{-}H_2O]^{2+}$ at m/z = 296.5721 (100%) (see Experimental Section and Fig. S43, SI).

3.3. DNA-metal compound interactions study

Due to the nature of an ongoing research project in which we are

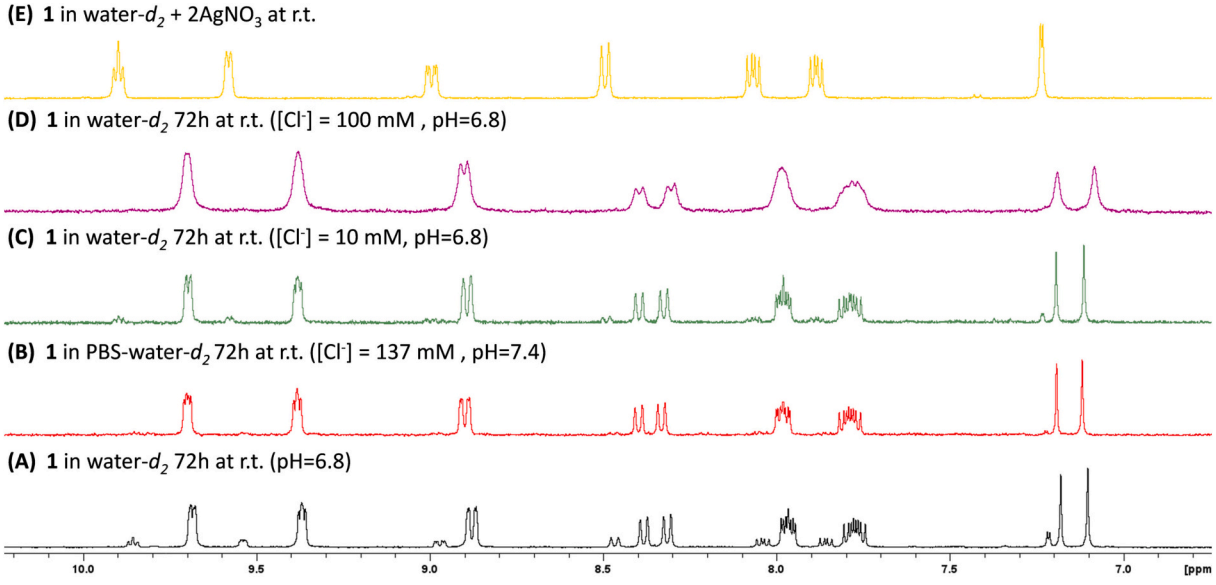

Fig. 3. Comparison of the aromatic region of ^{1}H NMR spectra of compound **1** in water-d_2, under different conditions.

involved [48–50], we were interested in knowing whether carbohydrate scaffolds in Ru(II) complexes can help to recognize DNA structures. Thus, different experiments were carried out to evaluate the possible interaction between compounds **1**–**5** and DNA. The techniques used included fluorescence-based (FRET) DNA melting temperature assays, viscosity titrations and equilibrium dialysis.

DNA FRET-melting assays were performed first to determine whether the compounds exert a stabilizing effect on DNA secondary structure due to partial or classical intercalation, most likely involving the heteroaromatic phenanthroline ring of the glycosylamine ligand.

First, the different metal-glycoconjugates **1**–**4** and compound **5** were tested with duplex-forming oligonucleotide F10T using a range of [ligand]/[DNA] ratios between 5 and 50 and a buffering system containing lithium chloride (100 mM). Under these experimental conditions, none of the metal complexes was able to modify the melting temperature of the DNA (see Fig. S44, SI). However, when the analogous experiments were carried out for selected metal glycoconjugates and aglycone **5** in non-saline buffered solution, the compounds were found to thermally stabilize the double helix, in a dose-dependent fashion (Figs. S45 and S46). The increase in Tm appears to be dependent on the nature of the carbohydrate and is not affected by differences in incubation times, up to 16 h. As the stabilization effect can be observed in complex **5**, lacking the carbohydrate moiety, but is not detected in cisplatin metallo-drug, we can conclude that our compounds, like complex **5** [41], are binding DNA, under these conditions, by a mechanism compatible with at least partial intercalation of the 1,10-phenanthroline ring.

DNA viscosity titrations were additionally performed to further investigate the binding mode of compounds **1–5** with CT dsDNA. This method allows to distinguish DNA intercalation from groove binding or electrostatic external binding to the phosphate backbone [51].

Compounds **1–4** presented a $(\eta/\eta_0)^{1/3}$ versus *r* linear correlation, and barely altered the DNA relative viscosity, showing only a slight decrease at increasing compound concentrations (Fig. S47, SI). The averaged slope values obtained are -0.248 ± 0.003 (**1**), -0.191 ± 0.004 (**2**), -0.233 ± 0.030 (**3**), and -0.250 ± 0.006 (**4**). Slopes in the range -0.3 to 0.2 are correlated with groove binding compounds and/or external electrostatic binding, while classical intercalants results in a slope close to 1.0 [51–53]. The aglycone **5** showed a slight decrease in DNA viscosity as well, but the $(\eta/\eta_0)^{1/3}$ versus *r plot* deviated from linearity. The fact that compound **5** is prone to form aggregates in aqueous buffered solutions could partially explain its distinctive effect on DNA viscosity. Compared to cisplatin metallodrug [54], the metal-glycoconjugates **1–4** do not induce significant conformational changes on DNA structure.

The combined results from FRET melting assays and viscosity titrations, without the addition of chloride ions, discard strong interactions with DNA, in particular, a classical intercalation binding mode. At the same time, at [LiCl] of 100 mM, compounds **1–4** most likely bind DNA through the grooves or by electrostatic interactions with the phosphate backbone.

Equilibrium dialysis experiments were also performed to determine CT DNA binding affinity of compounds **1–5**, in comparable conditions to that employed in viscosity titrations. For this purpose, we followed an adaptation of the protocol described by Chaires [55] (Experimental section). This allowed the determination of apparent association constants (K_{app}) shown in Table 1.

All apparent association constants determined were in the order of 10^4 M^{-1}, representing a modest binding affinity to dsDNA of metal compounds **1**–**5**. Within this series of compounds, the mannose derivative **2** displayed the highest binding constant, followed by the rhamnose **3** and the xylose metal-glycoconjugate **4**, whereas the glucose derivative displayed the lowest DNA affinity under the experimental conditions tested. Compound **5** was found to bind dsDNA with similar affinity than the metal-glycoconjugates. All in all, our in vitro DNA interaction studies indicate that, under the tested conditions, only minor differences were observed between glycoconjugates **1–4** and compound **5**, indicating that the presence of the carbohydrate moiety is not playing a determining role in DNA recognition.

Table 1
DNA apparent association constants of ruthenium(II) compounds **1**–**5** obtained by equilibrium dialysis[a].

Compound	1	2	3	4	5
K_{app} DNA CT (M^{-1}) x 10^{-4}	2.0 ± 0.2	3.1 ± 0.1	2.8 ± 0.1	2.6 ± 0.1	2.2 ± 0.2

[a] Apparent association constants were calculated according to the equation $K_{app} = C_b/(C_f)(S_{total} - C_b)$ where C_b is the amount of metal complex bound, C_f is the free metal complex concentrations and S_{total} is DNA concentration (75 μM), in monomeric units (bp).

3.4. *In vitro cell studies*

The cytotoxic activity of pro-ligands **a-d**, novel compounds **1**–**4**, aglycon **5** and cisplatin was evaluated in PC-3, and non-tumorigenic RWPE-1 cell lines. In addition, the in vitro cytotoxicity of metal compounds **1**–**5** against PC-3 cells was tested in the presence of BAY-876 [43], a pharmacological inhibitor of GLUTs. The antiproliferative and antimetastatic ability of the compounds was assessed in the PC-3 cell line by means of clonogenicity, migration, and metalloproteinases expression assays, respectively.

3.4.1. *Cell viability assays*

The cytotoxic effect of pro-ligands **a-d**, novel metal compounds **1**–**4**, and reference compounds cisplatin and **5** were tested by monitoring their ability to inhibit cell growth of PC-3 cells using the MTT assay, and assessed as the IC_{50} values after 24, 48 and 72 h of treatment. The results showed that none of the evaluated compounds were toxic to PC-3 cells after 24 h or 48 h (Table 2 and Table S1, SI), exception made for aglycone **5** (IC_{50} 24 h = 10.65 ± 1.09 μM). After 72 h of incubation, pro-ligands **b-d** and compound **5** exhibit higher cytotoxicity than cisplatin (Table 2), while corresponding metal-based glycoconjugates **2–4** exert moderate to good cytotoxicities. Among them, the best activity was found for mannose conjugation in ruthenium compound **2.**

Table 2
IC_{50} values (μM) after incubation (72 and 24 h) of compounds **1**–**5**, pro-ligands **a-d** and cisplatin with human prostatic cancer PC-3 and non-tumorigenic RWPE-1 cell lines[a].

Compounds	PC-3	RWPE-1	SI[b]
1	142.3 ± 1.4 781.4 ± 1.3^{24h}	> 200	n.d.
2	13.22 ± 1.45 410.8 ± 1.2^{24h}	79.44 ± 1.15	6.01
3	35.55 ± 1.45 1746 ± 1^{24h}	112.3 ± 1.1	3.16
4	24.24 ± 1.48 242.5 ± 1.1^{24h}	74.51 ± 1.04	3.07
5	1.34 ± 1.11 10.65 ± 1.09^{24h}	16.00 ± 1.03	11.9
a	35.06 ± 1.11 > 100^{24h}	17.95 ± 1.06	0.51
b	1.69 ± 1.09 > 100^{24h}	4.84 ± 1.06	2.86
c	7.77 ± 1.07 > 100^{24h}	9.28 ± 1.02	1.19
d	3.93 ± 1.07 > 100^{24h}	4.68 ± 1.05	1.19
cisplatin	16.52 ± 1.05 > 100^{24h}	16.13 ± 1.01	0.98

n.d. not determined.
[a] Data are the mean ± S.E.M of at least four experiments.
[b] Selectivity Index calculated after 72 h of incubation with cells, (SI) = IC_{50} (RWPE-1)/IC_{50} (PC-3).

To evaluate the selectivity toward cancer cells, IC_{50} values were also assessed in the non-tumorigenic RWPE-1 cell line. Among the organic pro-ligands, only **b** shows certain selectivity (SI = 3). The best selectivity indexes of metal derivatives are reached by metal aglycone **5** (SI = 12) and glycoconjugate **2** (SI = 6), suggesting that the metal plays a significant role in the selectivity mechanism, while the sugar moiety has no beneficial effect on it.

For comparison purposes, we attempt to measure the partition coefficients (log*P*) of metal glycoconjugates **1**–**4** and **5**. However, the insolubility of Ru(II) glycoconjugates **1**–**4** in n-octanol precluded log*P* determination by the shake flask method. In contrast, aglycone **5** afforded a log*P* = −1.00 ± 0.08, indicative of a more lipophilic profile than cisplatin (*log*P = −2.27) [56]. Most likely, the high hydrophilicity of arene Ru glycoconjugates compared to **5** complicates their cell internalization by passive diffusion. The same has been recognized to be a feature shared by many glycoconjugates [3,4,6]. A preliminary comparison study of the cellular uptake of cytotoxic compounds **2**–**5** into PC-3 cells was performed by ICP-OES, after cells exposure to each complex for 24 h at a concentration of 500 μM. Under these conditions, the cytotoxicity of the compounds correlates well with the Ru content being higher for **5**, followed by **2**, **4** and **3** (see Fig. S48, SI).

The clonogenic assay is a useful in vitro experiment to evaluate the ability of cancer cells to recover after treatment with a cytotoxic drug [57,58]. The assay tests every cell in a population for its ability to survive and to grow into a colony after exposure to an external agent for a short period of time. To test the potential effect that metal compounds **1**–**5** could have on colony formation, PC-3 cells were incubated for 24 h with the compounds at concentrations corresponding to their IC_{50} (24 h) values (Table 2). After treatment, the medium was replaced, and cells were maintained for further 14 days.

Results (Fig. 5) show that, under these conditions, Ru(II) glycoconjugates **1**–**4** inhibit PC-3 colony formation more potently than aglycone **5** (colony formation in compound-treated PC-3 relative to untreated control cells (100%) of 29.9% **1**, 27.4% **2**, 28.6% **3**, 27.45% **4** and 65.4% **5**, respectively), and demonstrate the cytostatic potential of the novel Ru(II) glycoconjugates.

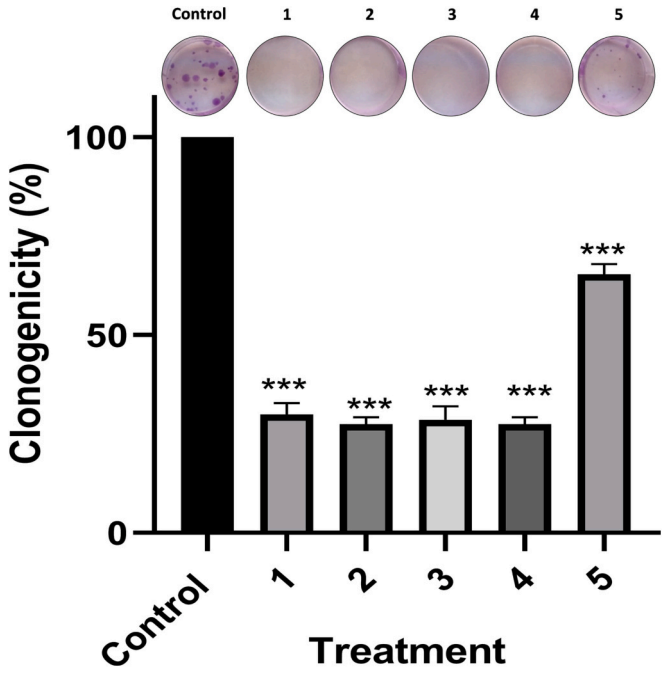

Fig. 5. Colony formation (after 15 days) of PC-3 cells pre-incubated with metal compounds **1**–**5** at their IC_{50}^{24h} for 24 h, relative to untreated control cells. Representative images of the assay and percentage of colonies formed vs control, values represent mean ± SEM of three independent experiments; ***, $P < 0.001$ vs Control.

These ruthenium compounds are, in general, more cytotoxic than the sugar modified analogues of RAPTA-C described by Hanif et al. [33], which were reported as moderately cytotoxic after 96 h of exposure to a variety of cell lines. A detailed study on the influence of the arene on the cytotoxicity and uptake of a variety of Ru(II) compounds containing a carbohydrate-phosphite ligand demonstrated the high influence that lipophilicity exerts on both properties [28,59]. In contrast, glycoconjugates containing cyclopentadienyl Ru(II) compounds [9,35,38], or carbonyl Ru(II) clusters [9], among others, have mostly been found to be highly cytotoxic.

It is well recognized that GLUTs, especially GLUT-1 and GLUT-3, are overexpressed in several human tumors, including prostate cancers such as PC-3 [60]. GLUT-facilitated cellular internalization of metal glycoconjugates has been indirectly evaluated before by comparison of the cell cytotoxicity of metal glycoconjugates in the presence or absence of GLUTs inhibitors (GLUTi) [34,39,61].

By this means, PC-3 cells were incubated with compounds **1**–**5** at their IC_{50} (72 h) concentration, in the presence or absence of GLUTi BAY-876 [43,62] and cell viability was assessed (Fig. S49, SI).

While control cells decrease their viability by a 13% in the presence of GLUTi BAY-876, the cells treated with this GLUTi and compounds **2**–**4** showed slight although statistically significant increments on the cell viability relative to the observed in the absence of BAY-876 (11.01% **2**, 13.34% **3** and 12.24% **4**, respectively, Fig. S49, SI). IC_{50} (72 h) of compound **2** was calculated in presence of an excess of the GLUTi (10 nM). The results showed a two fold increase of the IC_{50} under GLUT inhibitory conditions (IC_{50} + BAY-876 = 30.54 ± 1.07). However, in comparison with the values obtained for related glycoconjugated platinum compounds where GLUT-facilitated uptake has been demonstrated [34,36], the small differences found in our experiment do not allow us to elucidate whether GLUTs are involved in the transport of our ruthenium glycoconjugates inside the cell. In addition, the Ru content of PC-3 cells incubated with compound **2** (IC_{50}(24 h)) for 24 h in the absence or presence of GLUTi (2 nM) was quantified by Inductively Coupled Plasma Optical Emission spectroscopy (ICP-OES). Under the conditions used, no significant differences were found (592 ng/mL **2** + GLUTi and 562 ng/mL **2**).

3.4.2. *Wound-healing assay*

Impact of drug candidates on features related with cell-cell or -extracellular matrix (ECM) interactions, such as cell adhesion and migration are considered as markers for in vivo antimetastatic activity. Within this context, cell-migration is an important process involved in metastasis progression, and the wound-healing assay is a useful method for determining the in vitro antimigratory effect of drug candidates on cancer cells [24].

The method is based on quantifying the rate at which cells repopulate an artificial scratch created in a confluent monolayer of cells, in the absence or presence of the drug, and under conditions that do not cause cell death. Compounds **1**–**5** were then tested at their $IC_{50}/2$ (24 h) values (see Table 2). Under such conditions, the scratch made on untreated cells was almost fully repopulated after 24 h (Figs. 6 and 7A, 94.77% ± 1.9 of wound area closure), while the wound on cells incubated with metal compounds **1**–**5** shows an area closure relative to control cells of 23.4% ± 2.2 **1**, 19.3% ± 2.6 **2**, 16.6% ± 1.3 **3** and 28.7% ± 2.3 **4**, and 74.1% ± 4.4 **5**. The poorer inhibition performed by compound **5** relative to **1**–**4** on PC-3 cell migration seems to indicate that the presence of the carbohydrate is a requisite for the effect accomplished by the ruthenium glycoconjugates.

To evaluate the antimigratory potency of the compounds at lower concentrations, as well as the contribution of the metal center, we performed the experiment in the presence of **1**–**4** and pro-ligands **a**-**d** at 100 μM. The high cytotoxicity of **5** under these conditions precluded its inclusion in this assay. Under such conditions, pro-ligands **a**-**d** showed a slight to no-significant effect on PC-3 cells migration, (Figs. 7B and S50,

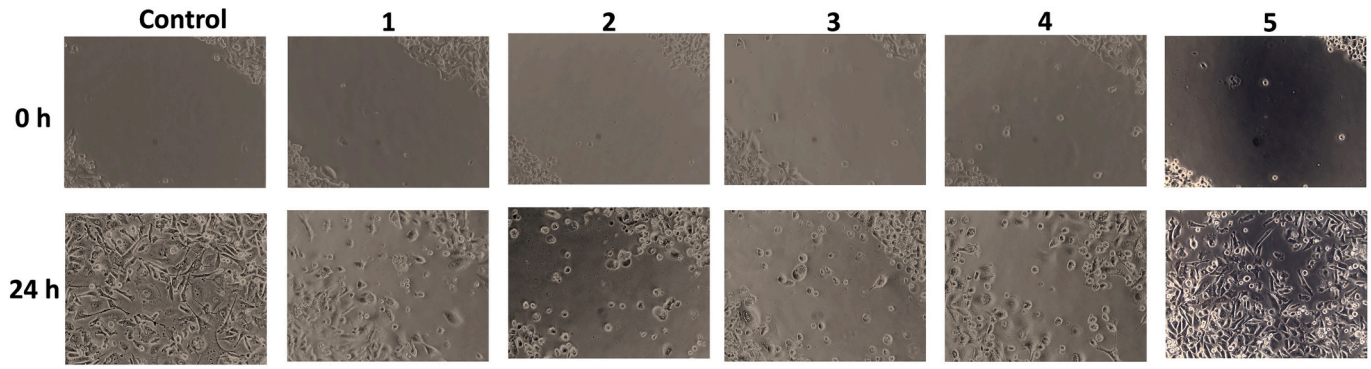

Fig. 6. Representative images of the wound healing assay. Effect of glycoconjugates **1**–**4** and aglycone **5** at their IC_{50}(24 h)/2 concentrations on wound area closure of PC-3 cells relative to untreated cells, at 0 and 24 h of treatment.

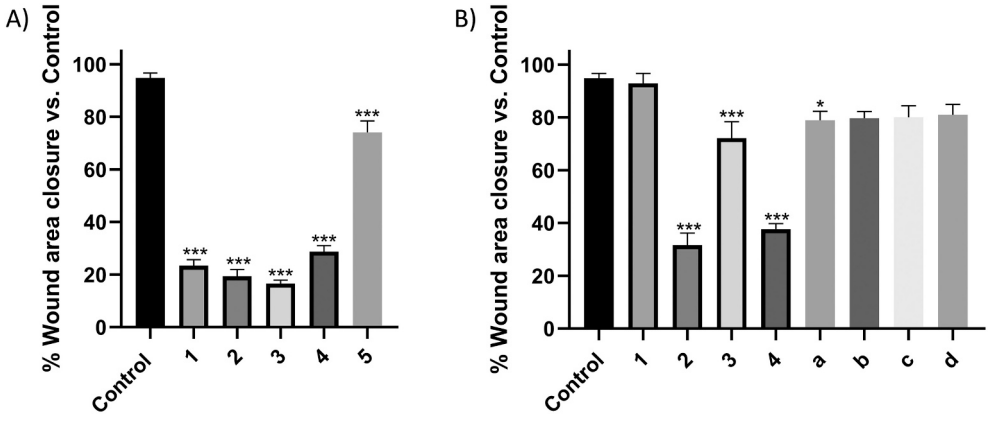

Fig. 7. A) Effect of metal glycoconjugates **1**–**4** and aglycone **5** at their IC_{50}(24 h)/2 concentrations and **B)** Effect of metal glycoconjugates **1**–**4** and ligands **a-d** at 100 μM on wound area closure of PC-3 cells relative to untreated cells, after 24 h of incubation. Microscopic analysis of the cell-free areas was carried out at 0 and 24 h after the addition of the drug and the width of the area invaded by prostate cells was estimated. Data are the mean ± SEM of at least four experiments. ***, $P < 0.001$ vs Control.

78.91% ± 3.4 **a**, 79.6% ± 2.5 **b**, 80.02% ± 4.4 **c**, 81.01% ± 3.9 **d**), while metal glycoconjugates **2**–**4** still cause an important decrease in the wound area closure relative to control cells, especially compounds **2** and **4** (31.6% ± 4.6 **2**, 72.2% ± 6.2 **3**, 37.7 ± 2.1 **4**).

These results indicate that along with the carbohydrate, the metal center plays a key role in the anti-migratory activity of Ru(II)-glycoconjugates.

In analogous in vitro migration assays, NAMI-A decrease limph node prostatic adenocarcinoma LNCaP cell migration by ca. 30% (10 μM) [63], while RAPTA-C reduces in a ca. 50% the closure of a scratch made on vascular endothelial ECRF-24 cells (200 μM) [64]. To the best of our knowledge, there are two other reported Ru(II)-glycoconjugates that have shown in vitro inhibition of cell migration. The arene compound [Ru(η^6-arene-carbohydrate)Cl(η^5-cyclopentadienyl)]Cl reported by Lamač et al. [40], inhibit migration of triple negative human breast cancer MDA-MB-231 and ovarian cancer SK-OV-3 cells by a 30–20% at ca. 200 μM, while the Ru(II) cluster $Ru_3(CO)_{11}$(L) (L = glucose-modified bicyclophosphite ligand), published by Nazarov et al. [29] decreased by about 60% the wound closure on MDA-MB-231 cells, at concentrations so low as 0.1 μM.

3.4.3. *Effect on MMPs activity*

Matrix metalloproteinases (MMPs) are a family of zinc- dependent endopeptidases that have been recognized as the major proteolytic enzymes for regulating ECM degradation [65,66]. Gelatinases MMP-2 and -9 are most commonly reported to be dysregulated in prostate cancers, among others, and are considered to play an essential role in tumour progression and related processes such as migration, invasion and angiogenesis. Within this context, the search for MMP's inhibitors have attracted considerable attention in recent years as an attractive approach for cancer therapy and diagnose [66,67].

Since ruthenium glycoconjugates **2**–**4** had shown to affect cell migration, we decided to investigate whether MMP-9 and/or − 2 activity was also affected in their presence. Proteolytic activity of MMP-9 and pro-MMP-9, pro-MMP-2 (zymogens of MMP-9 and MMP-2, respectively) in PC-3 cells (incubated with and without glycoconjugates **1**–**4**) was semi quantitatively determined by optical densitometry of gelatin zymography bands.

At the concentration tested, (100 μM), all metal glycoconjugates **1**–**4** decreased strongly the activity of MMP-9 relative to the untreated cells, especially the xylose conjugate **4** (Fig. 8, Table 3), while a lower effect was observed on pro-MMP-9 or − 2 activities. Since the high cytotoxicity of compound **5** hampers its evaluation at this same concentration, the average of the reduction applied to the IC_{50}(24 h) values of compounds **1**–**4** to reach 100 μM was also applied to **5**. Under such conditions, derivative **5** (1.5 μM) does not exert a significant effect on the evaluated MMPs *(96.98% ± 2.89 MMP-9; 103.2% ± 2.69 proMMP-9; 113.5% ± 4.72 proMMP-2)*. Remarkably, pro-MMP-9 and -2 are secreted by tumour cells and released into the extracellular environment as latent pro-enzymes that require activation in the extracellular space [68]. Thus, these results agree well with metal compounds exerting their influence at the cell surface.

A direct comparison with the behaviour of other Ru(II) compounds is hindered by the different methodology and cell lines used in the existing bibliography, however, it is worth mentioning that a few Ru(II) MMP-9 inhibitors [69–73] have been reported since the pioneering research on NAMI-A (inhibitor of MMP-9 activity on TS/A cells with IC_{50} ca. 600 μM) [74].

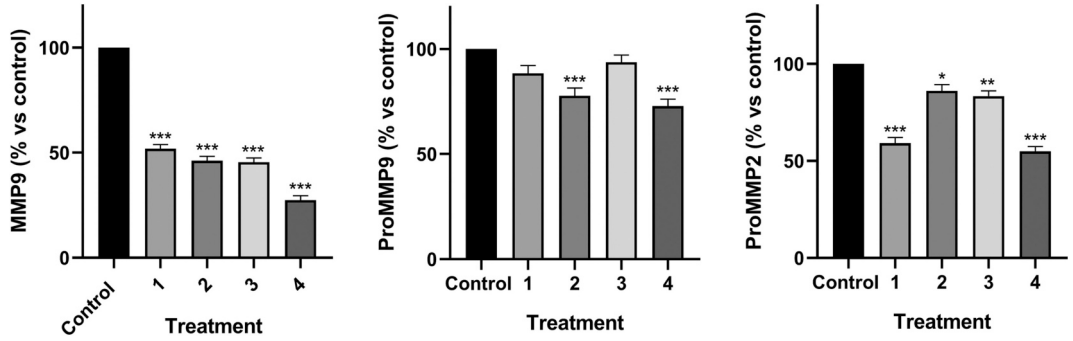

Fig. 8. Analysis of MMP-9, pro-MMP-9, and pro-MMP-2 activity in PC-3 cancer cells after treatment with the metal-compounds at 100 μM after 24 h of incubation. Data are the mean ± SEM of three independent experiments; *, $P < 0.05$; **, $P < 0.01$; ***, $P < 0.001$ vs Control.

Table 3
Percentage (%) of MMP-9, pro-MMP-9 and pro-MMP-2 activity relative to untreated cells (100%) in PC-3 cancer cells after treatment with metal-compounds **1**–**4** (100 μM). Data are the mean ± S.E.M of at least three experiments.

	MMP-9	ProMMP-9	ProMMP-2
1	51.84 ± 1.98	88.42 ± 3.77	59.14 ± 2.83
2	46.15 ± 2.06	77.75 ± 3.74	86.10 ± 3.19
3	45.49 ± 1.96	93.76 ± 3.41	83.35 ± 2.71
4	27.37 ± 2.12	72.82 ± 3.37	54.88 ± 2.50

4. Conclusions

We have established general access to novel carbohydrate-phenanthroline Ru(II) compounds **1**–**4**, which are water soluble and hydrolytically stable under physiologically relevant conditions. The characterization data collected confirm that the compounds are obtained as a mixture of epimers with ratios that depend on the specific glycoconjugate and the solvent used.

In addition, we carried out a comparative biological study between our novel compounds and the Ru(II) aglycone **5** reported before by Espino and García [41]. DNA interactions have been preliminarily studied for **1–4** by a variety of methods. The results confirm that DNA binding of the metal glycoconjugates is dependent on the buffer ionic strength. The metal glycoconjugates bind DNA with modest affinity in the minor groove and/or through external, electrostatic interactions in the presence of saline buffers, while depletion of chloride ions allows an interaction with dsDNA by a non-classical partial intercalation mechanism.

The high water solubility of glycoconjugates **1**–**4** relative to **5** prove how greatly glycoconjugation can influence lipophilicity. However, comparison of the MTT assays in the absence and presence of GLUTi BAY-876 points to a non-significant influence of GLUTs on the uptake of metal glycoconjugates. In addition, no evidence was found in our ruthenium glycoconjugates to support the idea that the presence of carbohydrate scaffolds improves the cytotoxic selectivity of the resulting drug.

Remarkably, research on processes and targets that do not necessarily involve cell internalization led to most promising data. Derivatives **1**–**4** have a clear anti-migratory potential on malignant cells and potently reduce MMP-9 activity and, to a lesser extent, MMP-2 and especially MMP-9 zymogens at concentrations of 100 μM. Due to their moderate cytotoxicity, the compounds could alter metastatic-related events at doses that do not cause significant cell death. Thus, the results ratify the compounds' adequacy for future in vivo assays in athymic mice.

Overall, the comparative assays performed have indeed confirmed that carbohydrate scaffolds substantially influence the biological effects exerted by our systems. In addition, preliminary results on the wound healing and MMPs activity assays, together with the shreds of evidence already reported for many organic glycoconjugates, support the driven hypothesis that metal drug-glycoconjugates can also affect some of the carbohydrate-binding protein interactions required in cancer progression and metastasis.

Author statement

E.T.-R. investigation, data curation, formal analysis, validation, visualization, methodology, writing original draft; L.M.-M. investigation, formal analysis, validation, supervision, writing - review and editing, A.M.B. supervision, resources, writing - review and editing, M.S. A.-P. investigation, conceptualization, supervision, writing - review and editing, T.C. supervision, writing - review and editing, L.G. conceptualization, methodology, validation, formal analysis, resources, supervision, funding acquisition, project administration, writing - review and editing, E.R. conceptualization, methodology, validation, supervision, funding acquisition, resources, project administration, writing - original draft.

Declaration of Competing Interest

The authors declare that they have no known competing financial interests or personal relationships that could have appeared to influence the work reported in this paper.

Data availability

I have shared a file with Supporting Information at the attach file step

Acknowledgments

Financial support from Ministerio de Ciencia e Innovación (PID2019-108251RB-I00/AEI/10.13039/501100011033), MINECO (CTQ2015-72625-EXP/AEI), Comunidad Autónoma de Madrid (CAM, I3 Program) and the Universidad de Alcalá (UAH, Projects UAH-AE-2017-2, PIUAH22/CC-028, CCG2020/CC-026, CCG2018-EXP-024, CCGP2017-EXP-019, CCG2015/BIO-010 and CCG20/CC-007) is acknowledged. A. M.B is grateful to Instituto de Salud Carlos III (ISCIII) and European Regional Development Fund (ERDF) for the P118/00526 grant. E.T.R. is grateful to Ministerio de Educación y Ciencia for the FPU19/03617 fellowship.

Appendix A. Supplementary data

Supplementary data associated with this article can be found in the online version, at http://. These data include: Representative NMR, UV–vis and HR-ESI MS spectra of compounds **1–4**. Selected biological data.

References

[1] O. Warburg, On the origin of cancer cells, Science 123 (80) (1956) 309–314, https://doi.org/10.1126/science.123.3191.309.

[2] E.C. Calvaresi, P.J. Hergenrother, Glucose conjugation for the specific targeting and treatment of cancer, Chem. Sci. 4 (2013) 2319–2333, https://doi.org/10.1039/c3sc22205e.

[3] A. Franconetti, O. Lopez, J.G. Fernandez-Bolanos, Carbohydrates: potential sweet tools against cancer, Curr. Med. Chem. 27 (2020) 1206–1242, https://doi.org/10.2174/0929867325666180719114150.

[4] J. Fu, J. Yang, P.H. Seeberger, J. Yin, Glycoconjugates for glucose transporter-mediated cancer-specific targeting and treatment, Carbohydr. Res. 498 (2020), 108195, https://doi.org/10.1016/j.carres.2020.108195.

[5] C. Reily, T.J. Stewart, M.B. Renfrow, J. Novak, Glycosylation in health and disease, Nat. Rev. Nephrol. 15 (2019) 346–366. https://www.nature.com/articles/s41581-019-0129-4.

[6] C. Hartinger, A. Nazarov, S. Ashraf, P. Dyson, B. Keppler, Carbohydrate-metal complexes and their potential as anticancer agents, Curr. Med. Chem. 15 (2008) 2574–2591, https://doi.org/10.2174/092986708785908978.

[7] G. Bononi, D. Iacopini, G. Cicio, S. Di Pietro, C. Granchi, V. Di Bussolo, F. Minutolo, Glycoconjugated metal complexes as cancer diagnostic and therapeutic agents, ChemMedChem 16 (2021) 30–64, https://doi.org/10.1002/cmdc.202000456.

[8] M. Gottschaldt, U.S. Schubert, Prospects of metal complexes peripherally substituted with sugars in biomedicinal applications, Chem. Eur. J. 15 (2009) 1548–1557, https://doi.org/10.1002/chem.200802013. WE - Science Citation Index Expanded (SCI-EXPANDED).

[9] A.C. Fernandes, Synthesis, biological activity and medicinal applications of ruthenium complexes containing carbohydrate ligands, Curr. Med. Chem. 26 (2019) 6412–6437, https://doi.org/10.2174/0929867326666190124124350.

[10] T.J. Boltje, T. Buskas, G.J. Boons, Opportunities and challenges in synthetic oligosaccharide and glycoconjugate research, Nat. Chem. 1 (2009) 611–622, https://doi.org/10.1038/nchem.399.

[11] C. Agatemor, M.J. Buettner, R. Ariss, K. Muthiah, C.T. Saeui, K.J. Yarema, Exploiting metabolic glycoengineering to advance healthcare, Nat. Rev. Chem. 3 (2019) 605–620, https://doi.org/10.1038/s41570-019-0126-y.

[12] F.-T. Liu, G.A. Rabinovich, Galectins as modulators of tumour progression, Nat. Rev. Cancer 5 (2005) 29–41, https://doi.org/10.1038/nrc1527.

[13] D. Compagno, L.D. Gentilini, F.M. Jaworski, I.G. Perez, G. Contrufo, D.J. Laderach, Glycans and galectins in prostate cancer biology, angiogenesis and metastasis, Glycobiology 24 (2014) 899–906, https://doi.org/10.1093/glycob/cwu055.

[14] Y. Nishimura, Gem-diamine 1-N-Iminosugars and related iminosugars, candidate of therapeutic agents for tumor metastasis, Curr. Top. Med. Chem. 3 (2003) 575–591, https://doi.org/10.2174/1568026033452492.

[15] P. Nangia-Makker, J. Conklin, V. Hogan, A. Raz, Carbohydrate-binding proteins in cancer, and their ligands as therapeutic agents, Trends Mol. Med. 8 (2002) 187–192, https://doi.org/10.1016/S1471-4914(02)02295-5.

[16] G. Sava, R. Gagliardi, A. Bergamo, E. Alessio, G. Mestroni, Treatment of metastases of solid mouse tumours by NAMI-A: comparison with cisplatin, cyclophosphamide and dacarbazine, Anticancer Res. 19 (1999) 969–972.

[17] C. Scolaro, A. Bergamo, L. Brescacin, R. Delfino, M. Cocchietto, G. Laurenczy, T. J. Geldbach, G. Sava, P.J. Dyson, In vitro and in vivo evaluation of ruthenium(II)-arene PTA complexes, J. Med. Chem. 48 (2005) 4161–4171, https://doi.org/10.1021/jm050015d.

[18] A. Bergamo, G. Sava, Linking the future of anticancer metal-complexes to the therapy of tumour metastases, Chem. Soc. Rev. 44 (2015) 8818–8835, https://doi.org/10.1039/C5CS00134J.

[19] G. Sava, A. Bergamo, Drug control of solid tumour metastases: a critical view, Anticancer Res. 19 (1999) 1117–1124.

[20] B.S. Murray, M.V. Babak, C.G. Hartinger, P.J. Dyson, The development of RAPTA compounds for the treatment of tumors, Coord. Chem. Rev. 306 (2016) 86–114, https://doi.org/10.1016/j.ccr.2015.06.014.

[21] M.A. Jakupec, M. Galanski, V.B. Arion, C.G. Hartinger, B.K. Keppler, Antitumour metal compounds: more than theme and variations, Dalton Trans. (2008) 183–194, https://doi.org/10.1039/b712656p. WE - Science Citation Index Expanded (SCI-EXPANDED).

[22] A. Bergamo, A. Masi, A.F.A. Peacock, A. Habtemariam, P.J. Sadler, G. Sava, In vivo tumour and metastasis reduction and in vitro effects on invasion assays of the ruthenium RM175 and osmium AFAP51 organometallics in the mammary cancer model, J. Inorg. Biochem. 104 (2010) 79–86, https://doi.org/10.1016/j.jinorgbio.2009.10.005.

[23] M.M. González-Ballesteros, C. Mejía, L. Ruiz-Azuara, Metallodrugs: an approach against invasion and metastasis in cancer treatment, FEBS Open Bio 12 (2022) 880–899, https://doi.org/10.1002/2211-5463.13381.

[24] M. Brindell, I. Gurgul, E. Janczy-Cempa, P. Gajda-Morszewski, O. Mazuryk, Moving Ru polypyridyl complexes beyond cytotoxic activity towards metastasis inhibition, J. Inorg. Biochem. 226 (2022), 111652, https://doi.org/10.1016/j.jinorgbio.2021.111652.

[25] Y. Li, B. Liu, H. Shi, Y. Wang, Q. Sun, Q. Zhang, Metal complexes against breast cancer stem cells, Dalton Trans. 50 (2021) 14498–14512, https://doi.org/10.1039/D1DT02909F.

[26] A. Pettenuzzo, K. Vezzù, M.L. Di Paolo, E. Fotopoulou, L. Marchiò, L.D. Via, L. Ronconi, Design, physico-chemical characterization and in vitro biological activity of organogold (iii) glycoconjugates, Dalton Trans. 50 (2021) 8963–8979, https://doi.org/10.1039/D1DT01100F.

[27] B. Banik, K. Somyajit, A. Hussain, G. Nagaraju, A.R. Chakravarty, Carbohydrate-appended photocytotoxic (imidazophenanthroline)-oxovanadium(iv) complexes for cellular targeting and imaging, Dalton Trans. 43 (2014) 1321–1331, https://doi.org/10.1039/C3DT52087K.

[28] M. Hanif, S.M. Meier, A.A. Nazarov, J. Risse, A. Legin, A. Casini, M.A. Jakupec, B. K. Keppler, C.G. Hartinger, Influence of the π-coordinated arene on the anticancer activity of ruthenium(II) carbohydrate organometallic complexes, Front. Chem. 1 (2013) 27, https://doi.org/10.3389/fchem.2013.00027.

[29] A.A. Nazarov, M. Baquié, P. Nowak-Sliwinska, O. Zava, J.R. Van Beijnum, M. Groessl, D.M. Chisholm, Z. Ahmadi, J. Scott McIndoe, A.W. Griffioen, H. Van Den Bergh, P.J. Dyson, Synthesis and characterization of a new class of anti-angiogenic agents based on ruthenium clusters, Sci. Rep. 3 (2013) 1–7, https://doi.org/10.1038/srep01485.

[30] C.T. Lau, C. Chan, K.Y. Zhang, V.A.L. Roy, K.K. Lo, Photophysical, cellular-uptake, and bioimaging studies of luminescent ruthenium(II)–polypyridine complexes containing a D-fructose pendant, Eur. J. Inorg. Chem. 2017 (2017) 5288–5294, https://doi.org/10.1002/ejic.201701038.

[31] M. Martinez-Alonso, G. Gasser, Ruthenium polypyridyl complex-containing bioconjugates, Coord. Chem. Rev. 434 (2021), 213763, https://doi.org/10.1016/j.ccr.2020.213736.

[32] I. Berger, M. Hanif, A.A. Nazarov, C.G. Hartinger, R.O. John, M.L. Kuznetsov, M. Groessl, F. Schmitt, O. Zava, F. Biba, V.B. Arion, M.S. Galanski, M.A. Jakupec, L. Juillerat-Jeanneret, P.J. Dyson, B.K. Keppler, In vitro anticancer activity and biologically relevant metabolization of organometallic ruthenium complexes with carbohydrate-based ligands, Chem. Eur. J. 14 (2008) 9046–9057, https://doi.org/10.1002/chem.200801032.

[33] M. Hanif, S.M. Meier, W. Kandioller, A. Bytzek, M. Hejl, C.G. Hartinger, A. A. Nazarov, V.B. Arion, M.A. Jakupec, P.J. Dyson, B.K. Keppler, From hydrolytically labile to hydrolytically stable RuII–arene anticancer complexes with carbohydrate-derived co-ligands, J. Inorg. Biochem. 105 (2011) 224–231, https://doi.org/10.1016/j.jinorgbio.2010.10.004.

[34] M. Patra, T.C. Johnstone, K. Suntharalingam, S.J. Lippard, A potent glucose-platinum conjugate exploits glucose transporters and preferentially accumulates in cancer cells, Angew. Chem. Int. Ed. 55 (2016) 2550–2554, https://doi.org/10.1002/anie.201510551.

[35] P.R. Florindo, D.M. Pereira, P.M. Borralho, C.M.P. Rodrigues, M.F.M. Piedade, A. C. Fernandes, Cyclopentadienyl-ruthenium(II) and iron(II) organometallic compounds with carbohydrate derivative ligands as good colorectal anticancer agents, J. Med. Chem. 58 (2015) 4339–4347, https://doi.org/10.1021/acs.jmedchem.5b00403.

[36] J. Ma, H. Liu, Z. Xi, J. Hou, Y. Li, J. Niu, T. Liu, S. Bi, X. Wang, C. Wang, J. Wang, S. Xie, P.G. Wang, Protected and de-protected platinum(IV) glycoconjugates with GLUT1 and OCT2-mediated selective cancer targeting: demonstrated enhanced transporter-mediated cytotoxic properties in vitro and in vivo, Front. Chem. 6 (2018) 386, https://doi.org/10.3389/fchem.2018.00386.

[37] R. Liu, Z. Fu, M. Zhao, X. Gao, H. Li, Q. Mi, P. Liu, J. Yang, Z. Yao, Q. Gao, GLUT1-mediated selective tumor targeting with fluorine containing platinum(II) glycoconjugates, Oncotarget 8 (2017) 39476–39496, https://doi.org/10.18632/oncotarget.17073.

[38] P.R. Florindo, D.M. Pereira, P.M. Borralho, P.J. Costa, M.F.M. Piedade, C.M. P. Rodrigues, A.C. Fernandes, New [(η 5 -C 5 H 5)Ru(N–N)(PPh 3)][PF 6] compounds: colon anticancer activity and GLUT-mediated cellular uptake of carbohydrate-appended complexes, Dalton Trans. 45 (2016) 11926–11930, https://doi.org/10.1039/C6DT01571A.

[39] M. Wenzel, A. de Almeida, E. Bigaeva, P. Kavanagh, M. Picquet, P. Le Gendre, E. Bodio, A. Casini, New luminescent polynuclear metal complexes with anticancer properties: toward structure–activity relationships, Inorg. Chem. 55 (2016) 2544–2557, https://doi.org/10.1021/acs.inorgchem.5b02910.

[40] M. Lamač, M. Horáček, L. Červenková Šťastná, J. Karban, L. Sommerová, H. Skoupilová, R. Hrstka, J. Pinkas, Harmless glucose-modified ruthenium complexes suppressing cell migration of highly invasive cancer cell lines, Appl. Organomet. Chem. 34 (2020) 1–5, https://doi.org/10.1002/aoc.5318.

[41] J. Valladolid, C. Hortigüela, N. Busto, G. Espino, A.M. Rodríguez, J.M. Leal, F. A. Jalón, B.R. Manzano, A. Carbayo, B. García, Phenanthroline ligands are biologically more active than their corresponding ruthenium arene complexes, Dalton Trans. 43 (2014) 2629–2645, https://doi.org/10.1039/C3DT52743C.

[42] K. Duskova, L. Gude, M.-S. Arias-Pérez, N-phenanthroline glycosylamines: synthesis and copper(II) complexes, Tetrahedron 70 (2014) 1071–1076, https://doi.org/10.1016/j.tet.2013.12.044.

[43] H. Siebeneicher, A. Cleve, H. Rehwinkel, R. Neuhaus, I. Heisler, T. Müller, M. Bauser, B. Buchmann, Identification and optimization of the first highly selective GLUT1 inhibitor BAY-876, ChemMedChem 11 (2016) 2261–2271, https://doi.org/10.1002/cmdc.201600276.

[44] H. Brunner, Stability of the metal configuration in chiral-at-metal half-sandwich compounds, Eur. J. Inorg. Chem. 2001 (2001) 905–912, https://doi.org/10.1002/1099-0682(200104)2001:4<905::aid-ejic905>3.0.co;2-v.

[45] M.G. Mendoza-Ferri, C.G. Hartinger, R.E. Eichinger, N. Stolyarova, K. Severin, M. A. Jakupec, A.A. Nazarov, B.K. Keppler, Influence of the spacer length on the in vitro anticancer activity of dinuclear ruthenium-arene compounds, Organometallics 27 (2008) 2405–2407, https://doi.org/10.1021/om800207t.

[46] Y. Fu, R. Soni, M.J. Romero, A.M. Pizarro, L. Salassa, G.J. Clarkson, J.M. Hearn, A. Habtemariam, M. Wills, P.J. Sadler, Mirror-image organometallic osmium arene iminopyridine halido complexes exhibit similar potent anticancer activity, Chem. Eur. J. 19 (2013) 15199–15209, https://doi.org/10.1002/chem.201302183.

[47] T.C. Johnstone, K. Suntharalingam, S.J. Lippard, The next generation of platinum drugs: targeted Pt(II) agents, nanoparticle delivery, and Pt(IV) prodrugs, Chem. Rev. 116 (2016) 3436–3486, https://doi.org/10.1021/acs.chemrev.5b00597.

[48] P. Gratal, M.-S. Arias-Pérez, L. Gude, 1H-imidazo[4,5-f][1,10]phenanthroline carbohydrate conjugates: synthesis, DNA interactions and cytotoxic activity, Bioorg. Chem. 125 (2022), 105851, https://doi.org/10.1016/j.bioorg.2022.105851.
[49] K. Duskova, S. Sierra, M.S. Arias-Pérez, L. Gude, Human telomeric G-quadruplex DNA interactions of N-phenanthroline glycosylamine copper(II) complexes, Bioorg. Med. Chem. 24 (2016) 33–41, https://doi.org/10.1016/j.bmc.2015.11.037.
[50] S. Jäger, L. Gude, M.-S. Arias-Pérez, 4,5-Diazafluorene N-glycopyranosyl hydrazones as scaffolds for potential bioactive metallo-organic compounds: synthesis, structural study and cytotoxic activity, Bioorg. Chem. 81 (2018) 405–413, https://doi.org/10.1016/j.bioorg.2018.08.019.
[51] D. Suh, J.B. Chaires, Criteria for the mode of binding of DNA binding agents, Bioorg. Med. Chem. 3 (1995) 723–728, https://doi.org/10.1016/0968-0896(95)00053-J.
[52] G. Cohen, H. Eisenberg, Viscosity and sedimentation study of sonicated DNA-proflavine complexes, Biopolymers 8 (1969) 45–55, https://doi.org/10.1002/bip.1969.360080105.
[53] T.A. Fairley, R.R. Tidwell, I. Donkor, N.A. Naiman, K.A. Ohemeng, R.J. Lombardy, J.A. Bentley, M. Cory, Structure, DNA minor groove binding, and base pair specificity of alkyl- and aryl-linked bis(amidinobenzimidazoles) and bis(amidinoindoles), J. Med. Chem. 36 (1993) 1746–1753, https://doi.org/10.1021/jm00064a008.
[54] E.R. Jamieson, S.J. Lippard, Structure, recognition, and processing of cisplatin−DNA adducts, Chem. Rev. 99 (1999) 2467–2498, https://doi.org/10.1021/cr980421n.
[55] J.B. Chaires, Structural selectivity of drug-nucleic acid interactions probed by competition dialysis, in: M.J. Waring, J.B. Chaires (Eds.), DNA Bind. Relat. Subj., Springer-Verlag Berlin, Berlin, 2005, pp. 33–53, https://doi.org/10.1007/b100441.
[56] I.V. Tetko, I. Jaroszewicz, J.A. Platts, J. Kuduk-Jaworska, Calculation of lipophilicity for Pt(II) complexes: experimental comparison of several methods, J. Inorg. Biochem. 102 (2008) 1424–1437, https://doi.org/10.1016/j.jinorgbio.2007.12.029.
[57] N.A.P. Franken, H.M. Rodermond, J. Stap, J. Haveman, C. van Bree, Clonogenic assay of cells in vitro, Nat. Protoc. 1 (2006) 2315–2319, https://doi.org/10.1038/nprot.2006.339.
[58] V.N. Sumantran, in: I.A. Cree (Ed.), Cellular Chemosensitivity Assays: An Overview BT - Cancer Cell Culture: Methods and Protocols, Humana Press, Totowa, NJ, 2011, pp. 219–236, https://doi.org/10.1007/978-1-61779-080-5_19.
[59] A.A. Nazarov, J. Risse, W.H. Ang, F. Schmitt, O. Zava, A. Ruggi, M. Groessl, R. Scopelitti, L. Juillerat-Jeanneret, C.G. Hartinger, P.J. Dyson, Anthracene-tethered ruthenium(II) arene complexes as tools to visualize the cellular localization of putative organometallic anticancer compounds, Inorg. Chem. 51 (2012) 3633–3639, https://doi.org/10.1021/ic202530j.
[60] P. Effert, A.J. Beniers, Y. Tamimi, S. Handt, G. Jakse, Expression of glucose transporter 1 (Glut-1) in cell lines and clinical specimens from human prostate adenocarcinoma, Anticancer Res. 24 (2004), 3057 LP – 3064, http://ar.iiarjournals.org/content/24/5A/3057.abstract, 3057 LP – 3064.
[61] A. Pettenuzzo, K. Vezzù, M.L. Di Paolo, E. Fotopoulou, L. Marchiò, L.D. Via, L. Ronconi, Design, physico-chemical characterization and in vitro biological activity of organogold(iii) glycoconjugates, Dalton Trans. 50 (2021) 8963–8979, https://doi.org/10.1039/d1dt01100f.
[62] M.K. Temre, A. Kumar, S.M. Singh, An appraisal of the current status of inhibition of glucose transporters as an emerging antineoplastic approach: promising potential of new pan-GLUT inhibitors, Front. Pharmacol. 13 (2022), https://doi.org/10.3389/fphar.2022.1035510.
[63] C. Mu, S.W. Chang, K.E. Prosser, A.W.Y. Leung, S. Santacruz, T. Jang, J. R. Thompson, D.T.T. Yapp, J.J. Warren, M.B. Bally, T.V. Beischlag, C.J. Walsby, Induction of cytotoxicity in pyridine analogues of the anti-metastatic Ru(III) complex NAMI-A by ferrocene functionalization, Inorg. Chem. 55 (2016) 177–190, https://doi.org/10.1021/acs.inorgchem.5b02109.
[64] P. Nowak-Sliwinska, J.R. Van Beijnum, A. Casini, A.A. Nazarov, G. Wagnières, H. Van Den Bergh, P.J. Dyson, A.W. Griffioen, Organometallic ruthenium(II) arene compounds with antiangiogenic activity, J. Med. Chem. 54 (2011) 3895–3902, https://doi.org/10.1021/jm2002074.
[65] K. Li, F.R. Tay, C.K.Y. Yiu, The past, present and future perspectives of matrix metalloproteinase inhibitors, Pharmacol. Ther. 207 (2020), 107465, https://doi.org/10.1016/j.pharmthera.2019.107465.
[66] A. Alaseem, K. Alhazzani, P. Dondapati, S. Alobid, A. Bishayee, A. Rathinavelu, Matrix metalloproteinases: a challenging paradigm of cancer management, Semin. Cancer Biol. 56 (2019) 100–115, https://doi.org/10.1016/j.semcancer.2017.11.008.
[67] S. Mondal, N. Adhikari, S. Banerjee, S.A. Amin, T. Jha, Matrix metalloproteinase-9 (MMP-9) and its inhibitors in cancer: a minireview, Eur. J. Med. Chem. 194 (2020), 112260, https://doi.org/10.1016/j.ejmech.2020.112260.
[68] R. Fridman, M. Toth, I. Chvyrkova, S.O. Meroueh, S. Mobashery, Cell surface association of matrix metalloproteinase-9 (gelatinase B), Cancer Metastasis Rev. 22 (2003) 153–166, https://doi.org/10.1023/A:1023091214123.
[69] P. Gajda-Morszewski, I. Gurgul, E. Janczy-Cempa, O. Mazuryk, M. Łomzik, M. Brindell, Inhibition of matrix metalloproteinases and cancer cell detachment by Ru(II) polypyridyl complexes containing 4,7-diphenyl-1,10-phenanthroline ligands—new candidates for antimetastatic agents, Pharmaceuticals 14 (2021) 1014, https://doi.org/10.3390/ph14101014.
[70] I. Gurgul, O. Mazuryk, M. Łomzik, P.C. Gros, D. Rutkowska-Zbik, M. Brindell, Unexplored features of Ru(II) polypyridyl complexes. Towards combined cytotoxic and antimetastatic activity, Metallomics 12 (2020) 784–793, https://doi.org/10.1039/d0mt00019a.
[71] Y. Wang, J. Jin, L. Shu, T. Li, S. Lu, M.K.M. Subarkhan, C. Chen, H. Wang, New organometallic ruthenium(II) compounds synergistically show cytotoxic, antimetastatic and antiangiogenic activities for the treatment of metastatic cancer, Chem. Eur. J. 26 (2020) 15170–15182, https://doi.org/10.1002/chem.202002970.
[72] A.B. Becceneri, A.M. Fuzer, A.M. Plutin, A.A. Batista, S.A. Lelièvre, M.R. Cominetti, Three-dimensional cell culture models for metallodrug testing: induction of apoptosis and phenotypic reversion of breast cancer cells by the trans -[Ru(PPh 3) 2 (N, N -dimethyl- N -thiophenylthioureato-k 2 O,S)(bipy)]PF 6 complex, Inorg. Chem. Front. 7 (2020) 2909–2919, https://doi.org/10.1039/D0QI00502A.
[73] J. Leskovská, N. Miklášová, P.M. Kubelac, P. Achimaș-Cadariu, J. Valentová, M. Markuliak, E. Fischer-Fodor, Antiproliferative ruthenium complexes containing curcuminoid ligands tested in vitro on human ovarian tumor cell line A2780, towards their capability to modulate the NF-κBTranscription factor, FGF-2 growth factor, and MMP-9 pathway, Molecules 27 (2022) 4565, https://doi.org/10.3390/molecules27144565.
[74] A.H. Velders, A. Bergamo, E. Alessio, E. Zangrando, J.G. Haasnoot, C. Casarsa, M. Cocchietto, S. Zorzet, G. Sava, Synthesis and chemical−pharmacological characterization of the antimetastatic NAMI-A-type Ru(III) complexes (Hdmtp) [trans- RuCl 4 (dmso-S)(dmtp)], (Na)[trans- RuCl 4 (dmso-S)(dmtp)], and [mer-RuCl 3 (H 2 O)(dmso-S)(dmtp)] (dmtp) = 5,7-Dimethyl[1,2,4]tr, J. Med. Chem. 47 (2004) 1110–1121, https://doi.org/10.1021/jm030984d.